U.S. DEPARTMENT OF THE INTERIOR

U.S. GEOLOGICAL SURVEY

MEASUREMENT OF SEISMIC P- AND S-WAVE ATTENUATION IN VOLCANIC TUFF, RAINIER MESA TUNNELS, NEVADA TEST SITE

By

R. D. Carroll[1]

Open-File Report 94-618

Prepared in cooperation with the
Defense Nuclear Agency

[1]Denver, CO

CONTENTS

ILLUSTRATIONS

ILLUSTRATIONS - Continued

ILLUSTRATIONS - Continued

TABLES

ABSTRACT

Ground shock measurements resulting from a nuclear explosion in P tunnel at the Nevada Test Site indicate attenuation rates somewhat greater than observed for events detonated in other tunnels in the Rainier Mesa area. Because ground shock attenuation is a factor in containment mechanisms, prediction of this phenomenon is of some importance. Published studies indicate that the properties having most influence on ground shock attenuation--gas voids and rock strength--directly and indirectly affect elastic wave attenuation in a significant manner and to a greater extent than they do compressional- and shear-wave velocities. Therefore, attenuations of shear and compressional waves were measured at two sites in P tunnel and at one site in N tunnel to determine if differences in elastic wave attenuation exist between the two environments, and to evaluate the technique for its utility as a qualitative tool for estimating comparative ground-shock attenuation at proposed event sites.

Spectral ratio, rise time, and time-domain amplitude techniques were used to reduce the data. The resulting values of Qp and Qs differ significantly between techniques. The data derived by the spectral ratio technique, considered most reliable, indicate greater attenuation at the P tunnel sites (Qp=18, Qs=18-23) than at N tunnel (Qp=23, Qs=35).

Uncertainties in the effects of scattering and interference, particularly at the N tunnel site, indicate that additional measurements are necessary to support these results and to develop the best technique for determining Q in this environment.

INTRODUCTION

Tunnels within the Rainier Mesa area at the Nevada Test Site have been sites of tests utilizing nuclear explosions for over three decades. Engineering features utilized to contain the radiation products of these explosions to the vicinity of explosion point rely to some extent on the magnitude of the shock wave energy generated by the explosion. At the P tunnel complex, wherein nuclear testing has been relatively recent (first test December, 1987), stress gages from the initial event in the U12p.02 drift indicate that the shock-wave energy was attenuated to a greater extent than observed in other tunnel complexes (Fig. 1). An investigation was undertaken to measure the elastic wave attenuation near the anomalous event site in P tunnel, and compare it with a similar measurement at N tunnel where the historical record of shock wave attenuation is not particularly anomalous. If differences in attenuation characteristics between sites could be demonstrated, this might provide a technique to evaluate the attenuation of the medium at other sites prior to site selection for a nuclear test. This obviously requires that

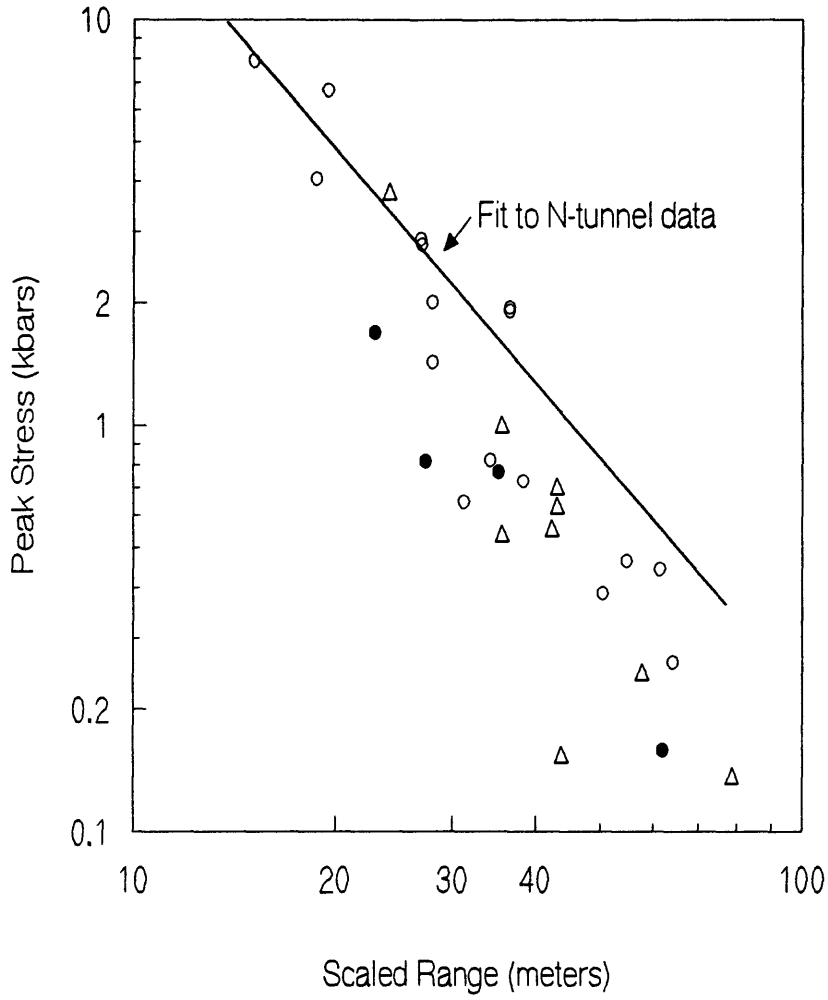

Figure 1.--Plot of shock wave attenuations measured in P tunnel. Solid circle, U12p.02 data; additional data from two events following U12p.02. Line of fit is for numerous events in N tunnel.

the elastic wave attenuation be sensitive to rock properties dominating shock wave attenuation. This report reviews these properties as they effect elastic wave attenuation and velocity, and describes the results of field investigations at two locations in P tunnel and at one location in N tunnel (Fig.2,3).

Geology of the Rainier Mesa area is described in detail elsewhere (Carroll and Magner,1988; Hoover and Magner,1990). The sites of interest are situated in bedded ash-fall tuffs of low to moderate dip; about 4° at the P tunnel sites and 18-20° at N tunnel. Drift alignment is approximately normal to the dip at P tunnel and subparallel at the N tunnel location.

General differences in physical setting and lithology between the two sites are illustrated in table 1 and on figure 4. The zeolitized tuffs at the two sites generally exhibit the same basic core properties, although the P tunnel site is located higher in the geologic section. In situ seismic velocities are slightly higher and overburden stress probably somewhat lower at the P tunnel site than at N tunnel. The greater thickness of densely welded tuff above P tunnel is not sufficient to overcome the difference in depths of burial between the two sites in equalizing the gravitational stress. Measurements of the stress state in Rainier Mesa for tunnels other than P have been published by Ellis and Magner (1980). The stress state at shallow depths can have a significant effect on seismic properties due to its influence on the state of closure of microcracks.

Other differences exist which may be postulated to have an effect on the seismic properties at the two sites. The tuffs in both tunnels are generally within a perched water zone, the regional water table occurring several hundred meters below the tunnels (Thordarson, 1965). Fractures in the tuff at the P tunnel site, however, are generally dry as opposed to N tunnel where many are saturated, suggesting that P tunnel is located above the zone of fracture saturation. Depending on the nature of the fractures, this difference can also significantly effect seismic properties.

Another difference lies in the nature of alteration of the tuff at the two sites. The perched water zone and high water retention of the tuffs is due to low permeability resulting from the zeolitization of vitric ash-fall tuffs. The transition zone delineating the boundary between zeolitized and non-zeolitized

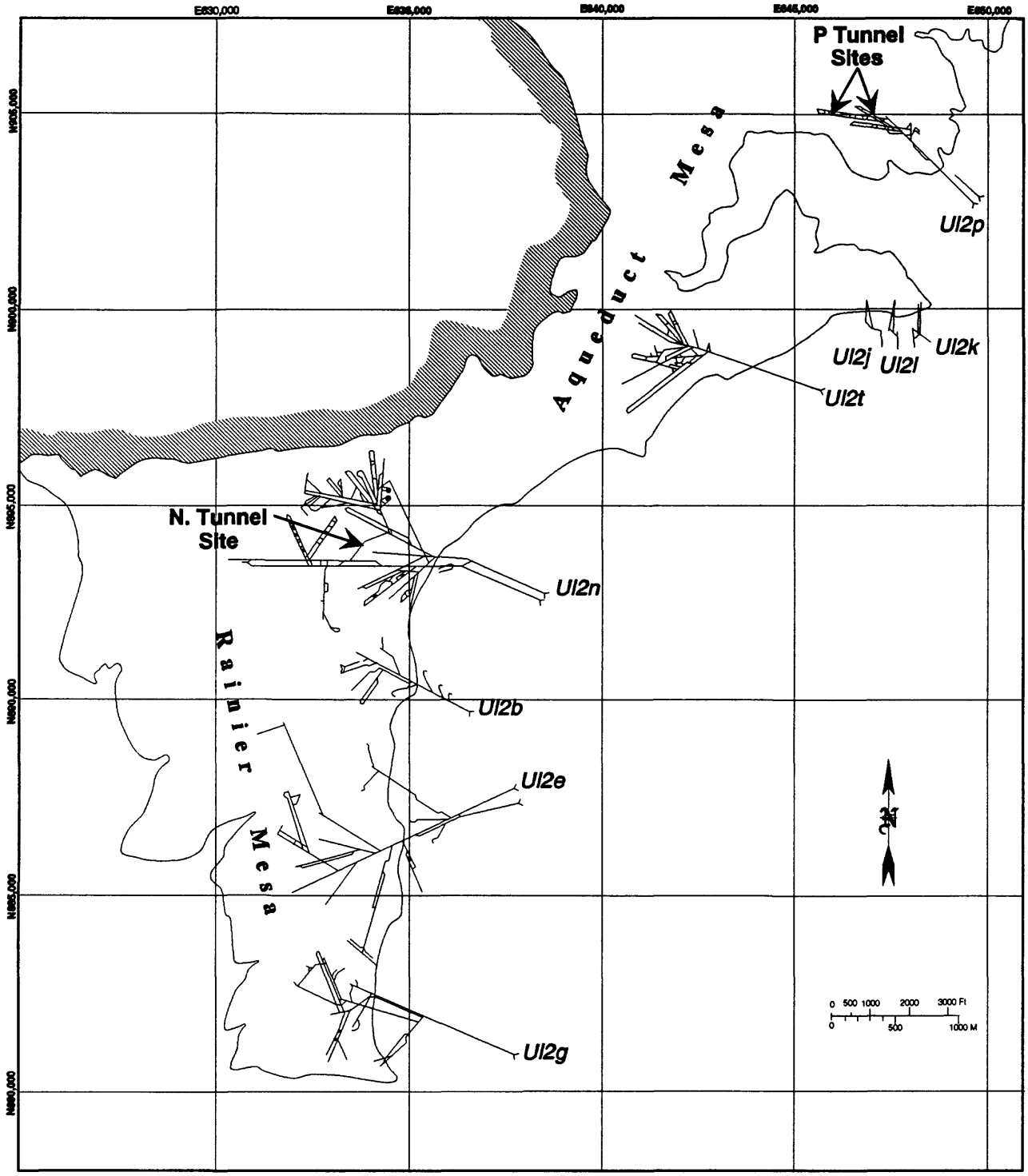

Figure 2. Map of Rainier Mesa area showing location of tunnel complexes and three sites at which attenuation measurements were made.

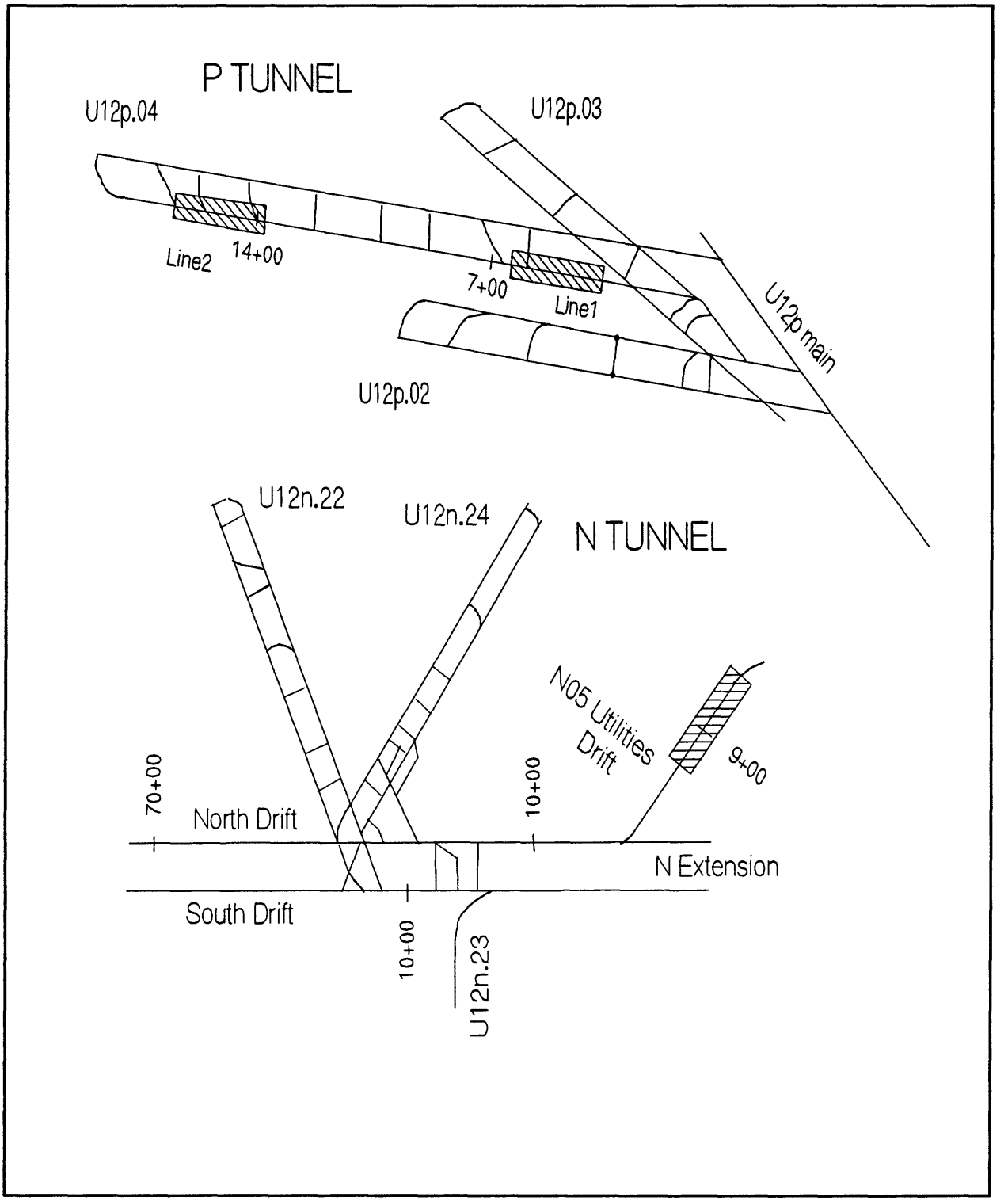

Figure 3.--Locations (shaded areas) of attenuation studies in P and N tunnels with respect to surrounding drifts.

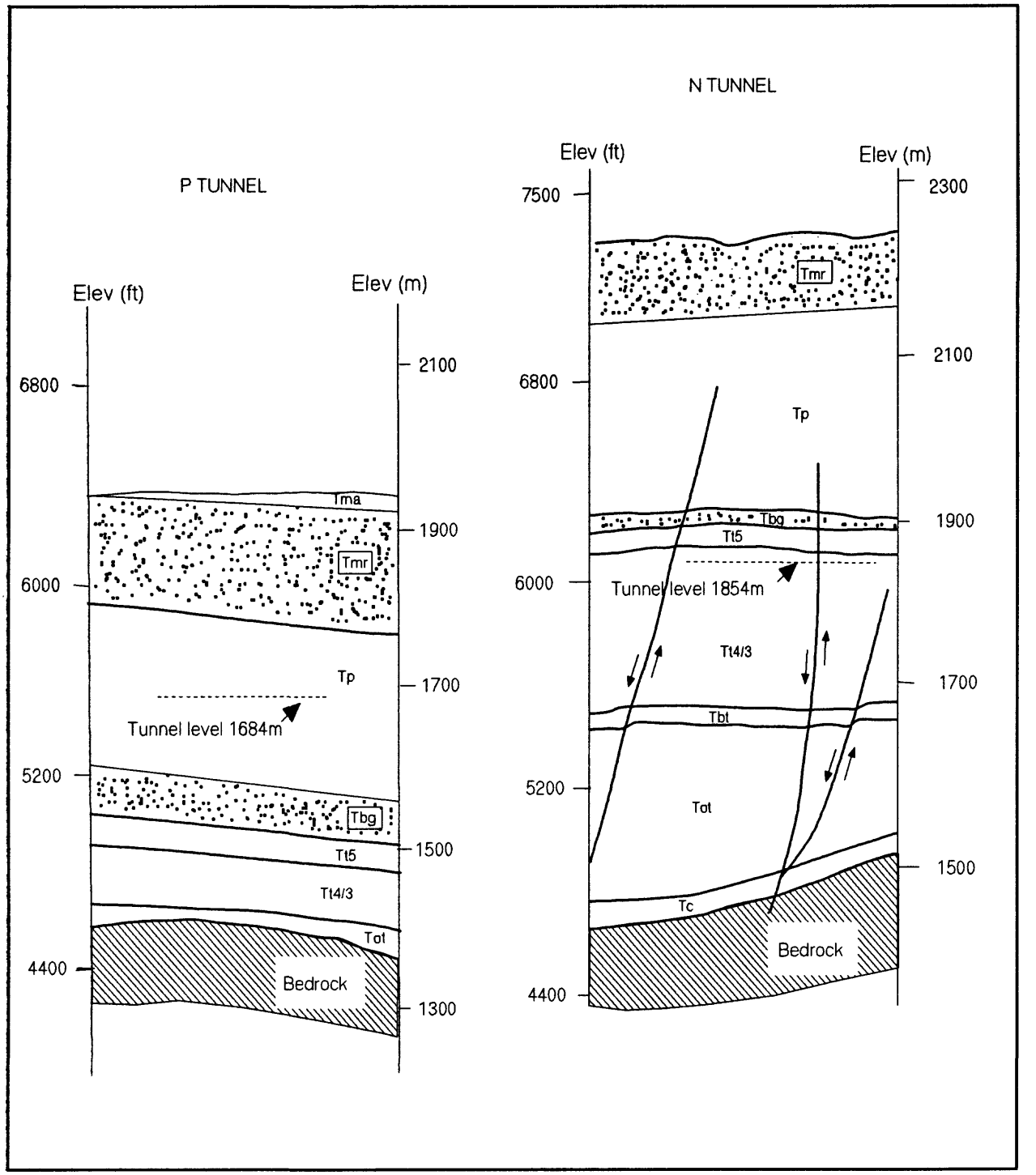

Figure 4.--Generalized geologic settings of P and N tunnel sites. Faulting at N tunnel known from geologic mapping. Extent of faulting below Grouse Canyon Member (Tbg) at P tunnel is unknown; faults are generally absent at tunnel level. Bedrock at P tunnel is dolomite; quartzite at N tunnel. (Geology after Raytheon Services Nevada).

Table 1.--Average properties of tuffs in vicinity of P and N tunnel sites.[1]

Density	1.9/2.0 gm/cc
Porosity	37/36 percent
Saturation	96/99 percent
P-wave velocity	2.9/2.7 km/s
S-wave velocity	1.4/1.1 km/s
Core P velocity	3.1/2.9 m/s
Overburden density	2.0/1.8 gm/cc
Grain density	2.4/2.4 gm/cc
Depth of burial	265/385 m

[1] First figure P tunnel, 2nd N tunnel. Data from n.24 and p.04 stemming regions. Velocities measured in-situ by Raytheon Services Nevada. Core data by Terra Tek Research.

tuffs is relatively sharp in P tunnel, ranging from 3 to 17 meters. (M. Baldwin, Raytheon Services Nevada, written commun; 1994). Estimates from geophysical logs in the region indicate that this zone may be as much as 55 m thick in some areas and less than a few meters thick in others (Carroll and Magner, 1988; Carroll, 1989). The mineralogic characteristics and, thus the elastic moduli, of the rocks on either side of the transition zone differ considerably, resulting in significant differences in seismic properties. Within the N tunnel complex the drifts are well within pervasively zeolitized tuff. The P tunnel complex, on the other hand, lies within or above the transition zone at some locations, and isolated zones of vitric tuff may occasionally be found in the zeolitized zone. This difference in mineralogy is locally offset by the presence of greater silicification in the P tunnel region, which may explain the somewhat higher seismic velocities observed. The core properties listed in table 1 apply to zeolitized tuffs near the explosion points. Saturations, densities, tuff strengths, and velocities are generally significantly lower in vitric tuff.

There is also a noticeable absence of mapped through-going faults in the P tunnel complex relative to N tunnel. This may be due to stratigraphic location and also may bear on the absence of fracture saturation. All these considerations raise questions concerning the relationship between structure, diagenetic alteration, and the hydrologic regime at the two sites. These considerations are not the major object of this investigation. They are pointed out because they imply that a significant difference in seismic attenuation may not be unreasonable between these two sites, the similarity of the core properties notwithstanding.

Of primary concern is the extent to which seismic attenuation relates to shock-wave attenuation at relatively short ranges from a nuclear explosion. The elastic strains involved in the seismic investigations discussed here are of the order of 10^{-6}, whereas, at the range of interest to containment studies, non-elastic strains many orders of magnitude in excess of this are typical. Thus the measured attenuations occur under circumstances in which the lithology is impacted by two significantly different dynamic processes. We are, however, interested in the rock properties which affect shock-wave attenuation and not necessarily the effects thereof. Consequently, it is more appropriate to determine if the rock properties which most strongly affect shock-wave attenuation can significantly affect elastic-wave attenuation. The properties of concern regarding shock-wave attenuation in the tuffs surrounding the Rainier Mesa tunnels are the air void content and rock strength. Air voids have a significant effect on seismic properties. Given strength variations between sites in Rainier Mesa, it is probable that air voids are the most significant property affecting shock wave attenuation. Rock strength is difficult to assess in situ, particularly with seismic methods; however, differences in strength due to fractures, porosity changes, and, in some cases, changes in matrix material, can be expected to strongly impact seismic properties. These relationships will be more fully explored in the next section.

Of additional utility is the extent to which seismic attenuation measurements provide insight into other areas of interest regarding the effects of nuclear explosions. Are attenuation measurements inherently more sensitive to bulk rock properties than are routine measurements of P- and S-wave velocity? One possible application lies in the determination of the range of shock damage arising from an underground nuclear explosion. In general, this can be accurately estimated from post-event observations of changes in shear-wave velocity (Carroll, 1983). However, there have been re-entry minebys near two nuclear events, Misty North and Husky Pup, where the measured shear-wave velocity was found to be only minimally affected at ranges where one normally expects significantly lower shear velocity compared to the velocity of undisturbed tuff. Can attenuation measurements provide increased sensitivity in such situations?

Another issue relates to the nature of the attenuation measurement itself. Examples of in situ measurements of attenuation at short ranges are relatively rare in the literature. Are the parameters involved in deriving attenuation measurements, given that they may provide more sensitivity than velocity measurements to rock properties, simply derived, or is the derivation technique subject to uncertainties which negate any increased sensitivity because of statistical uncertainties in the data (White, 1992)?

Before we proceed to these topics it is appropriate to introduce the general equation which governs elastic wave attenuation,

$$A=\frac{Ao}{R}e^{-\alpha R} \qquad (1)$$

where A is the amplitude of the seismic arrival observed at some distance R from the source, A_0 is the initial signal amplitude, and α is the attenuation coefficient. The most common measure of attenuation in rocks is the quality factor Q, or its inverse 1/Q, the dissipation factor. Q is related to the attenuation coefficient by,

$$\alpha=\frac{\pi f}{QV} \qquad (Q>1) \qquad (2)$$

where f is the propagation frequency and V the wave velocity (for a complete derivation see Bourbie and others, 1987, p.113; Hamilton, 1972). Q is the quantity sought at the three sites investigated in this report.

Several investigations are reported in the literature regarding the measurement of Q in the laboratory and in situ, and the assumptions and pitfalls involved in the measurement. Two of the more extensive compilations may be found in the Society of Exploration Geophysicists volume on attenuation edited by Toksoz and Johnston (1981) and in the text by Bourbie and others (1987). A detailed discussion of some of the procedures involved in a shallow in situ investigation has been reported by Redpath and others (1982).

In situ values for compressional-wave (Qp) and shear-wave attenuation (Qs) of rock can vary by nearly two orders of magnitude depending upon the measurement environment and the basic rock characteristics. Many of the published values of Q are for rock types, depths, and stress conditions not representative of the rock environment of concern in this study. They describe relatively deeply buried sandstones or igneous rocks of low porosity. For these rock types and environmental conditions, values of Q can be quite large compared to near-surface tuffs and sedimentary rocks. Q of rocks in near-surface environments is probably typically less than 30-40. Near-surface rocks exhibiting moderate to high porosities similar to the tunnel tuffs often exhibit Q values less than 20-30. Values of Q for rock types and conditions considered analogous to the ash-fall tuffs in the Rainier Mesa tunnels are listed in table 2 in addition to Q values for some standard materials. Values of Q for other rock types may be found in the references listed in the

table.

Attenuation measured in situ consists of two components, extrinsic and intrinsic attenuation. The intrinsic attenuation is generally considered the attenuation due strictly to the rock matrix and its associated components -- porosity, saturation, pore fluid, etc. The extrinsic attenuation results from extraneous mechanisms which affect the seismic amplitude because of geometric spreading of the wavefront, fractures, scattering and, refractions and reflections at impedance boundaries. For the purpose of defining differences in attenuation between tunnel sites it is desirable to include fractures in the intrinsic attenuation.

The presence of bedding in the tuff raises the question of refracted arrivals and their effect on the attenuation measurement. Although refracted data are routinely used to measure attenuation (Hatherly, 1986; Jongmans, 1990) we must be concerned with multiple refractions from bedding planes given the geometry of these investigations. Numerous refraction surveys obtained in tunnels within Rainier Mesa over several years rarely indicate refraction breaks in time-distance plots over the distances involved in this study (Carroll and Kibler, 1983). Although refraction theory is simple, the actual propagation of elastic waves in this environment, and many others, is complex as evidenced by the universal absence of purely radial compressional-wave motion in field refraction measurements. There is little doubt that arrivals at some locations are integrated effects of beds which are thin relative to the seismic wavelength. Vertical geophones were mainly used in these studies and arrivals obtained are considered a sample of the integrated intrinsic attenuation of the surrounding media. Thus, although losses due to some intrinsic effects are traditionally difficult to evaluate, it is assumed that over the short distances involved in our investigations these losses are not significant.

Acknowledgements

This work was performed under funding provided by the Defense Nuclear Agency. The efforts of Byron Ristvet and Barbara Harris-West, DNA in providing logistics for the field work are gratefully acknowledged. Geotechnical data regarding some aspects of the tunnel sites were obtained from Margaret Baldwin and Dean Townsend of Raytheon Services Nevada, and their efforts are much appreciated. The assistance of Dave Kibler, USGS, in the field measurement aspects of the investigation also merits commendation.

Table 2.--Velocity and attenuation data for selected samples.[1]

Sample[2]	Vp (km/s)	Vs (km/s)	Qp	Qs	Pressure[3] (MPa)	Porosity	Remarks[4]
Berea Sandstone	4.0 3.8	2.4 2.0	314 15	92 10	41 atm	19	Lab data; p. 25 p. 111, 113
Navajo Sandstone	4.1 4.0	2.5 2.3	63 7	28 6	10 2	13	Johnston and Toksoz (1980)
Boise Sandstone	3.4	1.9	7	6	atm	25	Lab data; p. 106
Pierre Shale	2.2	0.8	32 98	10	76-229 m 0-1219 m		In-situ data; p. 23 p. 263
Aluminum	6.3	3.1	5,900	17,200			Lab data; p. 124
Fresh water	1.48		210,000				Lab data; resonance, p. 124
Salt water	1.52		63,000				Lab data; resonance, p. 124
Air	0.343		3,465				Lab data; resonance, p. 124

[1] Some data extrapolated from plots in references.
[2] Rocks all under saturated conditions. Measurements by pulse technique except where noted.
[3] Pressure difference between frame and pore fluid. Pierre Shale data refer to depth of burial.
[4] Page numbers refer to Toksoz and Johnston (1981).

PROPERTIES AFFECTING Qp, Qs, and VELOCITY

The sensitivity of elastic-wave attenuation to rock strength and air void content, the properties of primary interest in shock-wave attenuation, and whether this sensitivity is greater than that offered by P- and S-wave velocity, may be evaluated from existing laboratory and theoretical studies. Although strength and seismic parameters are not directly related, inferences concerning differences in rock strength may be drawn from variations of seismic parameters with saturation, in situ stress, and interstitial and fracture porosity.

For the laboratory results to follow, only the data for samples near saturation are presented because this is the regime of interest in our investigations; saturations below about 50 percent are probably not realistic for Rainier Mesa subsurface rocks. Studies of attenuation near zero saturation are, however, informative regarding attenuation mechanisms and may be found in Toksoz and Johnston (1981). Data were assembled from various authors in order to examine the behavior of the same rock type for all measurements, in this case the Massilon sandstone which exhibits a porosity of about 23 percent. Jones (1983) reports P- and S-wave velocities for this lithology of about 3.5 km/s and 2 km/s at effective stresses near those at tunnel level in Rainier Mesa. Other experimenters report slightly different velocities (Nur and others, 1980; Murphy, 1982).

Many of the reported laboratory measurements were obtained by the resonance technique. Extensional velocity (Ve) and attenuation (Qe) obtained from bar resonant techniques differ from bulk values of P-wave velocity (Vp) and attenuation (Qp). Equations relating these values are available (Winkler and Nur, 1979; Murphy, 1984b), and these authors provide comparisons for measurements obtained using Massilon sandstone samples. Laboratory pulse measurements, the technique also used to obtain most of the available laboratory velocity data concerning Rainier Mesa tuffs such as listed in table 1, yield bulk values (Vp). For our purposes these differences are unimportant, and the trends displayed in the following plots may be considered an adequate representation of trends expected in in-situ measurements. Under some circumstances, because of frequency effects, differences between the two measurement techniques can be significant, particularly near full saturation. In such cases the bar resonance method appears to yield results in which trends are more akin to results expected under in situ seismic conditions (Murphy, 1984a).

Saturation

Figure 5 reproduces laboratory core data demonstrating the

behavior of extensional velocity, shear velocity, and attenuation as a function of saturation. Shear velocity is typically insensitive throughout the saturation range and compressional velocity only becomes sensitive in a narrow region near full saturation. Qp and Qs, on the other hand, are both sensitive near saturation, and the relative attenuations reverse at complete saturation, S-wave attenuation becoming greater than P-wave. At lesser saturations the P-wave attenuation is always greater than S-wave, significantly so in the region near full saturation. Measurements on dry and saturated samples (Toksoz and others, 1979) and dry, saturated, and partially saturated samples (Winkler and Nur, 1979) yield similar results.

Note further that the attenuation data are considerably more sensitive to saturation changes than are the velocity data in the region near saturation. The absence of sensitivity of shear-wave velocity arises from the relationship of shear velocity to shear modulus and density,

$$Vs=\sqrt{\frac{G}{\rho}} \qquad (3)$$

where, G is the shear modulus and ρ the density. The trivial decrease in shear velocity with saturation is due to the minor increase in density arising from the addition of saturant to the sample. Thus shear wave velocity, although highly diagnostic of shock wave damage in the Rainier Mesa tunnel environments, is quite insensitive to gas voids. The extensional velocity, however, undergoes a rather dramatic increase near saturation due to increased stiffening of the rock frame. The range of this increase is dramatic in some rocks. The change in extensional velocity near full saturation is estimated to be less than 15 percent for this sample. In the case of attenuation, on the other hand, there is a considerable effect from water saturation. The extensional attenuation increases about 50 percent near a saturation of 85 percent and decreases dramatically beyond that point. The extensional attenuation is always greater than the shear except at full saturation, where shear attenuation reaches a maximum and exceeds compressional wave attenuation. Shear attenuation for this sample increases by over 50 percent as one approaches saturation. Thus, attenuation is obviously a more sensitive measure of gas voids than is seismic velocity. The observation drawn from the foregoing studies that $Qp/Qs>1$ in fully saturated zones, and $Qp/Qs<1$ in partially saturated zones, is a tool of possible utility as a diagnostic for gas voids in the tuffs.

In Situ Stress

The relative sensitivity of seismic velocity and attenuation to

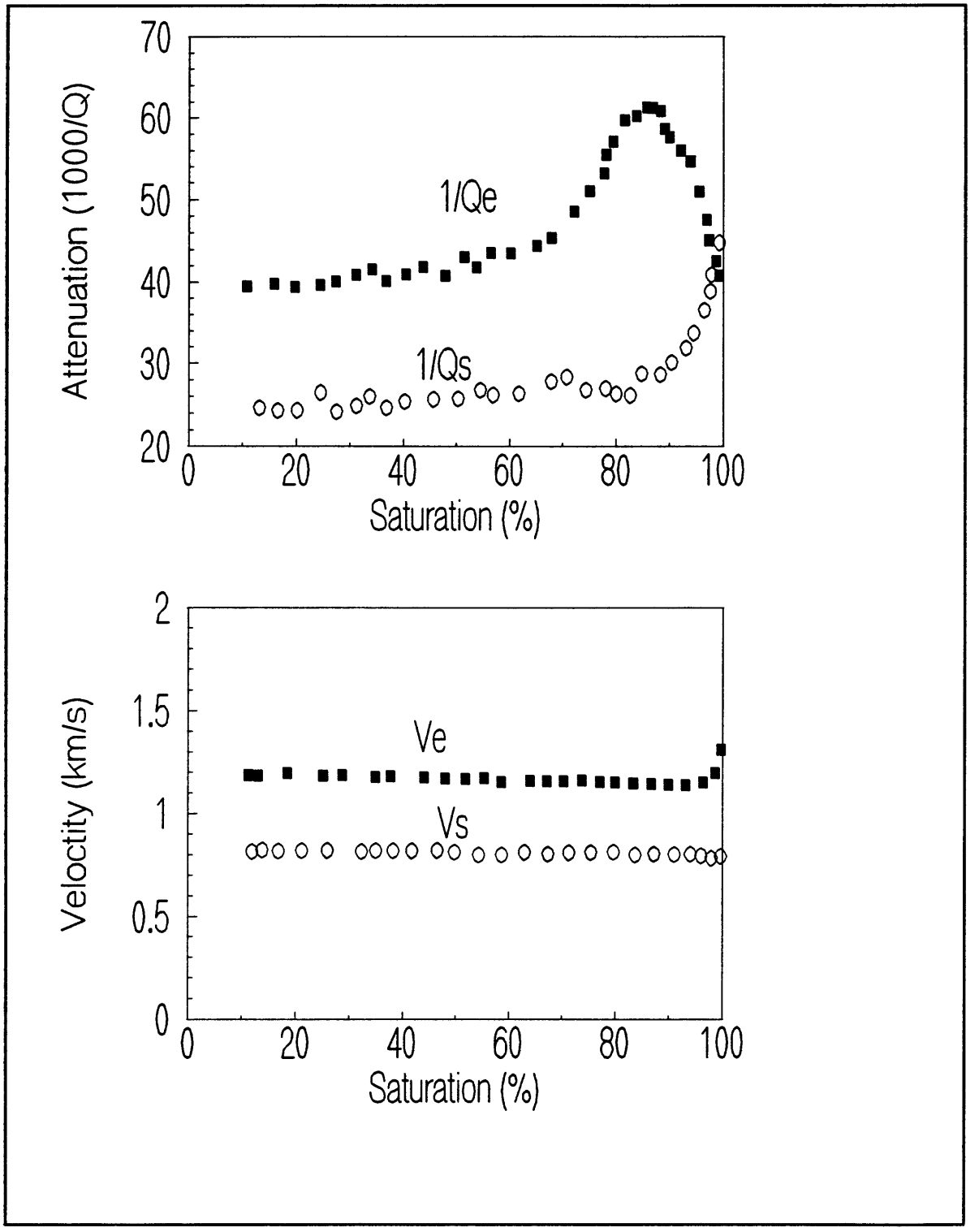

Figure 5.--Attenuation and velocity as a function of saturation for Massilon sandstone core samples. Not all experimental point are shown. Data by resonant bar technique under atmospheric conditions (Murphy, 1982).

effective stress (stress difference between pore fluid and rock frame) for samples of Massilon sandstone is compared on figure 6. It is again apparent that attenuation changes are, in general, significantly greater than changes in seismic velocity in response to stress changes. The stress state at tunnel level in Rainier Mesa is unbalanced, and little is known regarding pore pressure in the perched water environment of the tunnels. The maximum principal stress is generally less than 10 MPa (Ellis and Magner, 1980) and thus stress conditions at tunnel level occur in the region where both attenuation and velocity exhibit the greatest sensitivity to stress state. Relatively large changes of velocity and attenuation with stress (depth) is typical for most shallow rocks due to incomplete closure of microcracks and grain contacts. In general, attenuation is seen to exhibit greater sensitivity to pressure changes than is velocity.[1]

Fractures

The effect of fractures on seismic properties is extremely difficult to quantify experimentally. Consequently, conclusions are based upon theoretical treatments examining the seismic properties of a solid wherein the fractures are the only porosity in the material. For the Rainier Mesa tuffs at tunnel level, the matrix porosity makes up about one third of the volume of the rock and fractures are not extensive. Thus, the relative contribution of fractures to observed velocity and attenuation is difficult to assess, but is probably minor except at isolated locales where fractures occur in conjunction with silicification or other induration processes.

Figure 7 is a plot of the theoretical effect of fractures on velocity and attenuation for three crack porosities at a frequency of 100 Hz. For a description of the behavior predicted over a wide range of frequencies the original paper of O'Connell and Budiansky (1977) should be consulted. For the model assumed, these data indicate that the theoretical sensitivity of attenuation to fractures greatly exceeds that of velocity. Over the range of crack porosity represented, velocities change by less than a factor of two, whereas, attenuations change by an order of magnitude.

In summary, the foregoing examples demonstrate that attenuation

---

[1]The closure of microcracks and grain contacts under pressure may not be as dramatic in some tunnel tuffs as in other rocks. Measurements made by the author of velocity versus unconfined compression for 61 samples of saturated tuff from Tunnel Bed subunit 4F (velocity range 2.4 to 3.0 km/s) indicate a mean increase of only 3 to 6 percent in compressional velocity from atmospheric conditions to 7 MPa. The higher velocity tuffs exhibit smaller increases in velocity.

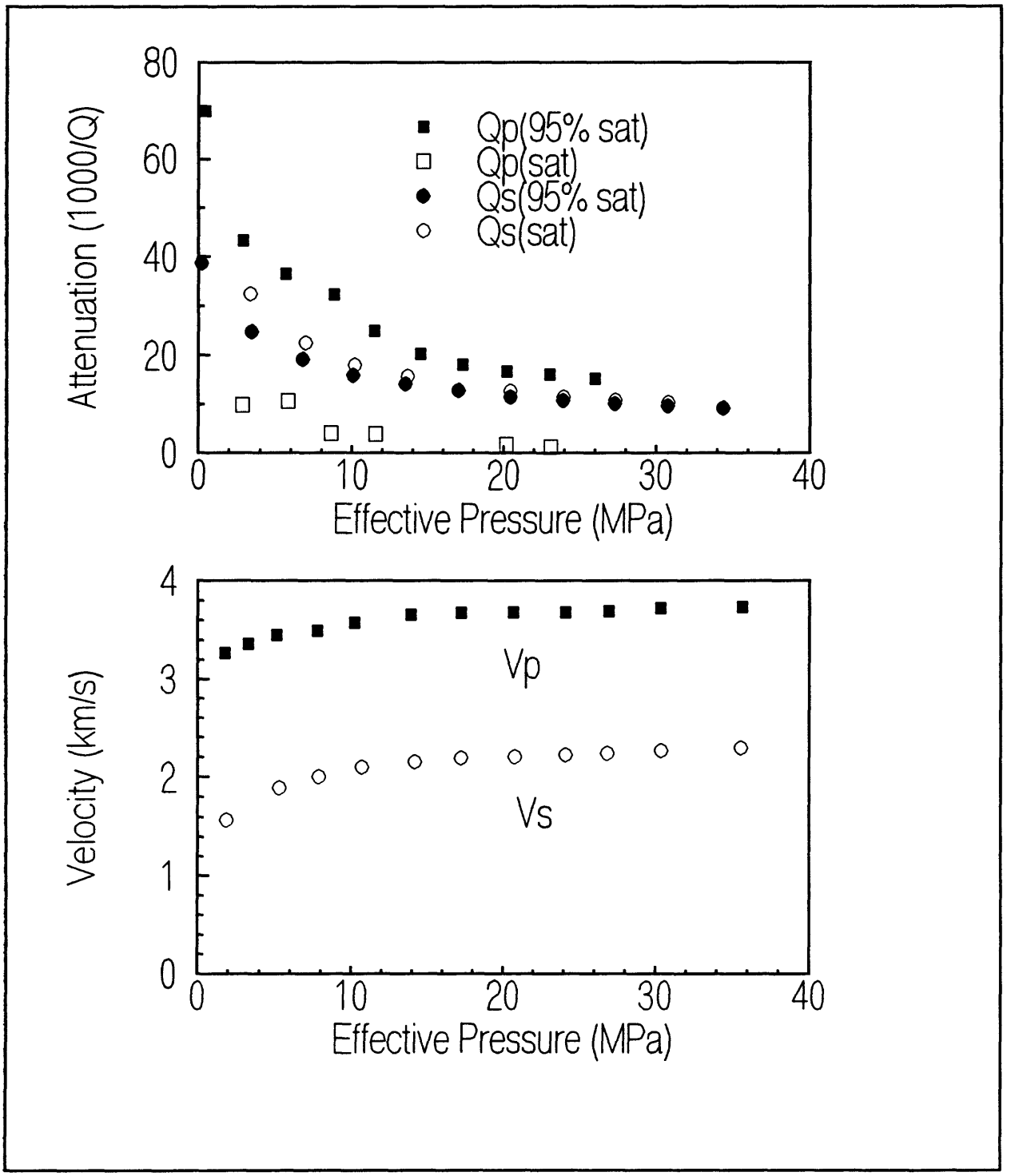

Figure 6.--Attenuation and velocity as a function of pressure for Massilon sandstone core samples. Not all experimental points are shown. Attenuation by resonant bar technique (Winkler and Nur, 1979). Velocity by pulse technique (Jones, 1983).

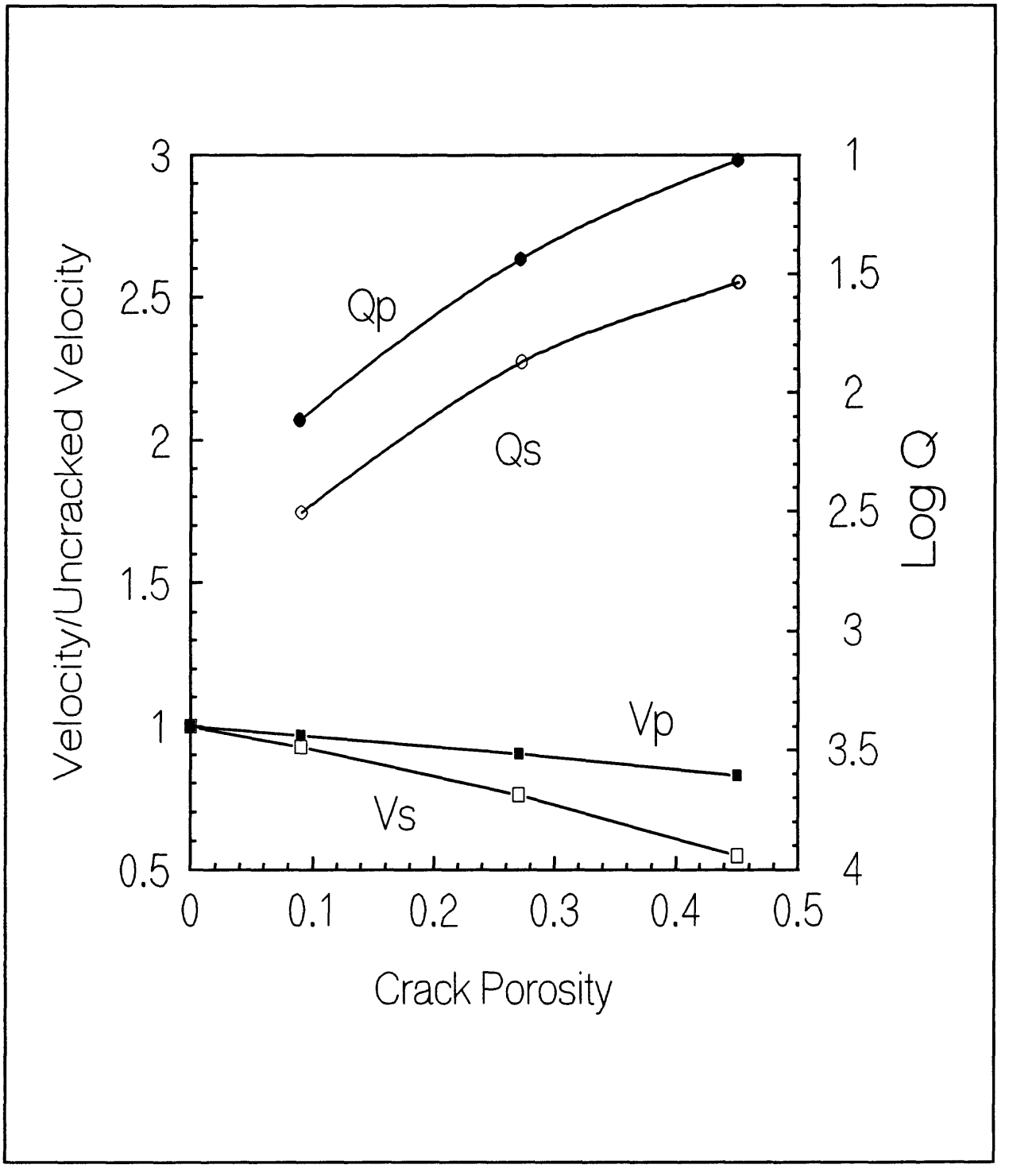

Figure 7.--Plots of ratio of cracked/uncracked P- and S-wave velocities and Qp, Qs as a function of crack porosity. Data points are for saturated crack porosities of 0.09, 0.27 and 0.45 extrapolated from figure 7 of O'Connell and Budiansky (1977) at a frequency of 100 Hz.

is considerably more sensitive than seismic velocity to the presence of gas voids and other rock properties from which strength might be indirectly inferred.[2] With regard to saturation and the detection of gas voids, attenuation may be more informative in some circumstances than P-wave velocity. Finally, it is difficult to imagine that any dramatic decrease in shock-wave attenuation due to changes in basic rock properties would not also result in noticeable changes in seismic attenuation.

MEASUREMENT TECHNIQUE

Figure 8 depicts the main components of the measurement system used at the two sites.

Recording System

The main system components consisted of an Acrosystems (now Analogic Devices) AT6400 waveform digitizer and Dolch PAC 286-12 portable computer. Six channels of data were acquired, the computer screen providing excellent resolution of the captured waveforms. The AT6400 is capable of 14 bit recording on 1,2,4, or 8 channels at a maximum rate sampling of 1 MHz. Sample rates ranged from 20 kHz with dynamite sources to 5 Khz for S-wave recording with mechanical sources. The maximum number of data points recorded was 2500 per channel. The minimum number was 1600. No anti-aliasing filters were employed, however, Fourier spectra indicate that these sample rates were more than adequate to prevent aliasing. Significant frequencies above 3 Khz were not observed with dynamite sources nor above 1 Khz with mechanical sources. Four input ranges are available, ranging from $\pm$125 mv to $\pm$8 volts full scale, thus providing LSB's of 15.625 uv to 1 mv. This has proven to be an excellent system, although in some instances, acquiring the first several cycles of the waveform without clipping required repeat shooting.

Data were recorded using sensors spaced at 15 m intervals. The

---

[2]We recognize some oversimplification regarding the gross characterization of bulk rock strength from seismic properties viz-a-viz ground shock attenuation. In addition to the presence of fractures and voids and their saturation state, seismic measurements can also be quite sensitive to the cohesion of matrix minerals, all of which have a large effect on bulk rock strength. However, at the large strains involved in ground shock, some unknown amount of attenuation occurs due to movement along fractures, faults, and bedding planes, i.e., induced block motion. Although seismic wave measurements are affected to various degrees by the presence of these discontinuities, they may bear little relation to the boundary conditions which control induced block motion from site to site.

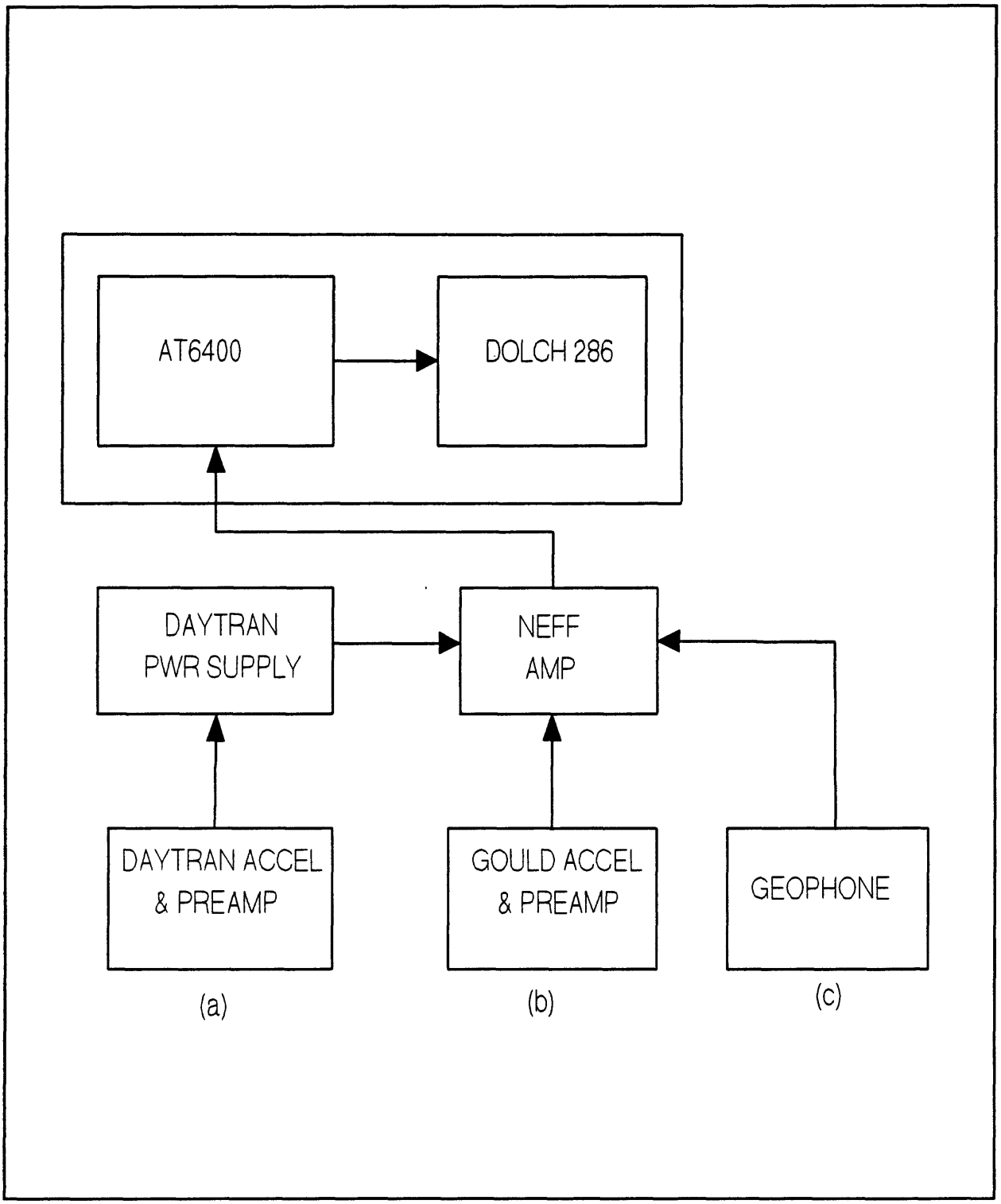

Figure 8.--Block diagram of equipment used in attenuation studies. a) and c) were used in P tunnel; b) and c) were used in N tunnel.

digitized signals were captured in the computer via an interface card providing 32 Kb of memory yielding 4 Kb of memory per channel. This provides about 200 milliseconds of data per channel at the maximum sampling rates used in this study. (Additional firmware allows streaming to disk for direct capture to memory, but was not required in this study.) Travel time for shear waves is about 70 milliseconds at the farthest station, and in some instances trigger delays were employed to examine later events. A geophone located near the source provided the trigger. The system may be triggered on any channel and in a variety of modes including pre and post trigger capture. A Diconix 150 Plus printer was used was used to obtain field printouts.

Software

Field data were acquired and manipulated using a HEM Data Corporation software package. This package contained all necessary software to address the AT6400 as well as providing for significant data processing capability. Sample rate, triggering, post-acquisition filtering, FFT, selectable display of channel(s), windowing, display expansion, cursor identification of channel coordinates, and other features necessary to adequate capture and condition the data are available. Programmable features allow for additional operations such as reject-or-keep stacking.

Although numerous operations in time and frequency domain can be obtained with this software, it was necessary to further output the time domain and Fourier transformed waveforms as ASCII files (via a HEM translator package). These were imported into a Cohort Software statistical and graphical software package to implement the more involved spectral and time domain operations necessary to obtain Q values and to plot the data.

Only one additional software component was used. This consisted of a WordPerfect macro programmed to strip selected statistical parameters (e.g., least-squares amplitude versus frequency fits) from Cohort files for further plotting and manipulation when using the spectral ratio technique.

Sensors

Cultural noise in the tunnels is often greater than exists for surface surveys, and signal-to-noise ratios are of concern. Our initial approach was to use accelerometers to record dynamite generated waveforms because of their greater frequency-amplitude response, and to use geophones with the lower frequency mechanical impact sources because of their greater sensitivity. At the P tunnel sites L-40A geophones and Daytran voltage-mode accelerometers were employed as sensors. The geophone mechanical and electrical resonances were checked for consistency in both vertical and horizontal modes. Manufacturer's specs regarding

frequency response were assumed correct. The Daytran accelerometers were individually calibrated by the manufacturer, providing 100 mv/g sensitivity, and amplitude fidelity within 2 percent to 5 Khz. A Model 4122 Daytran power supply provided current to the accelerometer impedance matching amplifiers. Six input channels with gains of 1, 10, 100 are also available. Signals were transmitted to the recording station via individual RG58/U cables. However, low signal-to-noise was a problem at the farthest accelerometer stations using the Daytran system.

At the N-tunnel site L-40A and L-25D geophones and Gould CA640516 accelerometers were utilized. The accelerometers were old voltage-mode types without built-in impedance matching amplifiers, however, recalibration indicated they were functional, providing about 37 mv/g output when operating with a 3 m cable into a pre-amplifier (gains 1 to 10, step 2.5) built in house. Response was flat within less than 2 percent to 5 Khz. The preamps were ganged with NEFF 128 amplifiers (maximum gain 1000). Bench tests indicated this system provided greater overall signal-to-noise ratios than the Daytran equipment.

Accelerometers and geophones were pre-cast in Sulfaset cylinders and then grouted in shallow drill holes. Geophone inserts were used with damping resistors soldered across the input terminals, and connections were waterproofed with Dow Corning #838 cement prior to casting.

Sources

Dynamites charges generally consisted of 1/4 to 1 stick of 40 percent dynamite. Larger charges (as much as 2 sticks) were sometimes required on Line 1 in P tunnel because of reduced sensitivity of the Daytran accelerometers. Because of the proximity of instrumentation cables associated with an upcoming nuclear test near the shotpoints on Line 2 in P tunnel, large charges were deemed imprudent and only geophone data were acquired.

Shear waves were obtained at both sites by grouting shear sledges in 1 m deep drill holes, 10.2 cm in diameter. The sledges consisted of "dumbbells" constructed from 3.2-cm diameter steel rods. Two 1.25-cm thick circular plates were affixed at each end, one end serving as a striking plate for a sledge hammer and the other serving to help anchor the sledge in the hole. The sledges were grouted in the hole with the upper impact plate extending about 10 to 15 cm above the tunnel invert at the hole collar. These proved to be excellent sources of SV energy.

A vacuum hammer was also employed at the N tunnel site. The hammer consists of a 43 kg weight impacting on an anvil under vacuum (Carroll and Magner, 1993). This is also an excellent SV wave generator. P-wave energy, however, is less successfully

generated with this device than with dynamite, but under proper noise conditions and with waveform stacking, the hammer provides a cleaner P wave.

MEASUREMENT LAYOUT

P Tunnel

The two P tunnel sites were situated in the U12p.04 bypass drift, U12p.02 having been rendered inaccessible by the nuclear test. The location of Line 1 (Figs. 3,9) was more critical than that of Line 2 for two reasons. First, it was desirable to locate the seismic line within lithology similar to that in the front end of the adjacent U12p.02 drift where the attenuated shock wave was measured. Secondly, it was necessary to avoid any effect on the data which might arise from locating the seismic line within tuff which had been fractured by the passage of the shock wave arising from the nuclear detonation. Geophysical and geologic evidence obtained in U12p.04 immediately after mining indicate shock damage to be restricted to the section between CS 8+50 and CS 10+50 (M. Baldwin, Raytheon Services Nevada, written commun., 1990).[3]

The sensors on Line 1 were located in pairs of vertical 7.6-cm diameter holes separated by about 1.2 meters. Holes 1.8 m deep were used to grout the Daytran accelerometers and geophones were grouted in the additional set of holes at a depth of 1 meter. With the exception of the shear source grouted in a 1 m depth hole, dynamite shot holes were all 1.8 m deep. The shear source was offset 5.2 m from the first sensor. Shot hole offsets ranged from 6 to 17 meters.

The location of Line 2 was somewhat compromised at the time of seismic measurements by construction underway for the upcoming U12p.04 nuclear event . An extensive cable bundle was exposed in the vicinity of the shot points in addition to a grout slab several cm thick in place along the tunnel invert. Locating any line closer to the proposed U12p.04 detonation point was negated by construction activities. It was considered desirable, however, to attempt to obtain data in the lithologic environment of this upcoming event for comparison with Line 1 within the U12p.02 lithologic setting.

On Line 2 the shear source was offset 6.7 m from the first sensor and the shot holes were offset from 6.1 to 6.9 meters. Only geophones were employed as detectors on this line.

---

[3]The closest approach in U12p.04 from the detonation in U12p.02 is about 56 m at CS 9+40 in U12p.04 (Fig. 3).

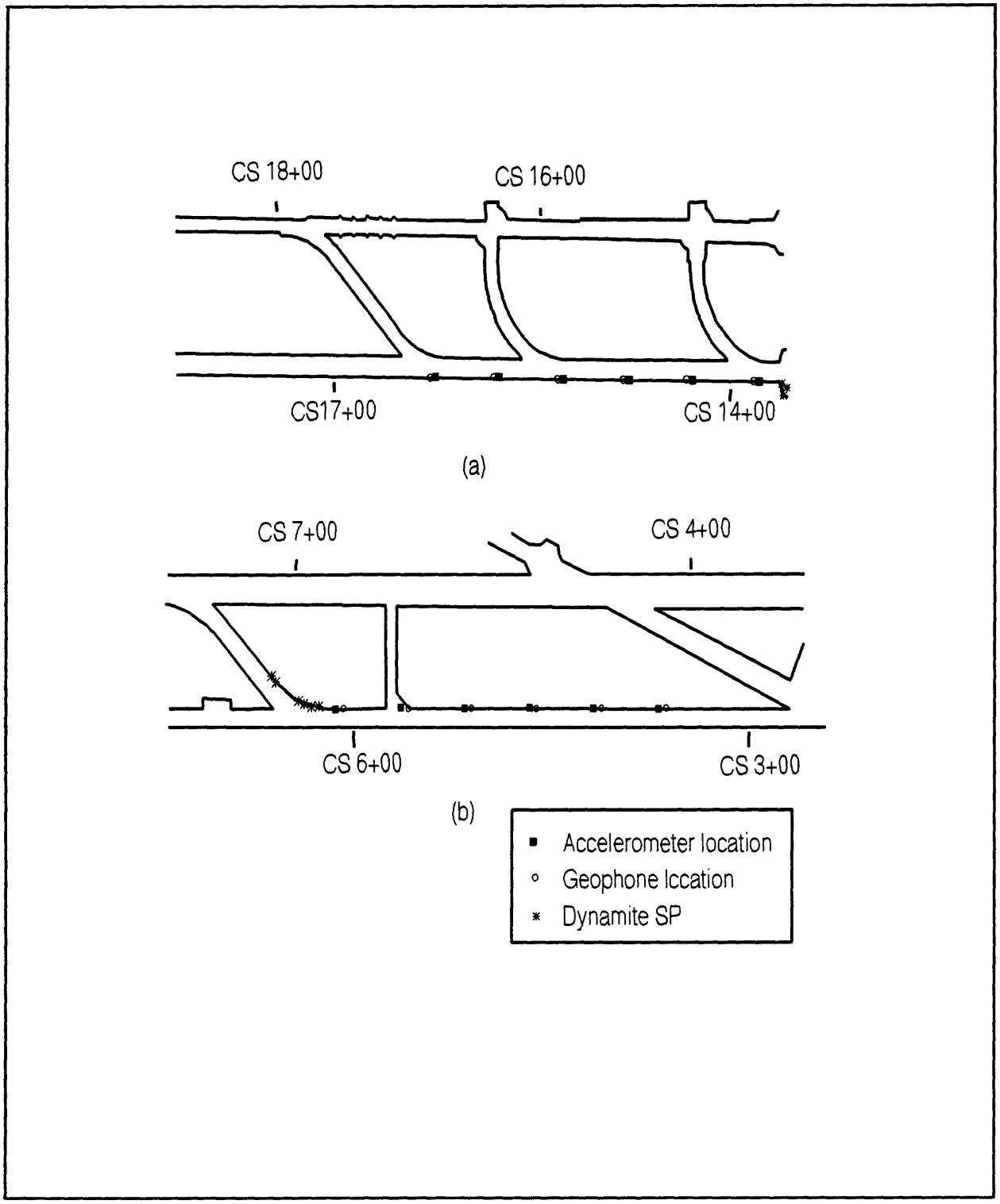

Figure 9.--Layout of seismic lines in U12p.04 bypass drift. a) Line 2-sensors in vertical holes between CS13+66 and CS16+05, and b) Line 1-sensors in vertical holes between CS3+66 and CS6+12.

N Tunnel

The seismic line in N tunnel was located in the U12n.05 Utilities Drift (Fig. 10). Within the extensive network of drifts in the N tunnel area, there are few locations where construction features such as drains, shotcreted invert and ribs, cables, and other construction features which might cause seismic waveform contamination, are not present. This was also true in the Utilities Drift, where a drain line was located beneath a layer of pea gravel along the rib chosen for the survey. (The opposite rib contained extensive electrical and air utility lines). Thus the sensors in N tunnel were located in the rib. The inclined drill holes contained grouted Gould accelerometers oriented to respond in-line with the tunnel axis. The preamplifiers were located at the hole collars. The deep (1.8 m) horizontal holes contained grouted L40a geophones oriented vertically. A package consisting of an in-line L25D geophone plus a L40-A geophone oriented transverse to the tunnel was placed in the 0.3 m holes. Unfortunately, half of the accelerometers used at this site failed, probably due to moisture.

DATA REDUCTION

There are several techniques for deriving Q from the recorded waveform, all subject to various degrees of accuracy dependent upon the circumstances of measurement (Tonn, 1989). Basically four methods are generally employed in shallow in-situ studies; the spectral ratio method, the rise time method, the time domain amplitude method, and the rise time-propagation technique. Several authors have compared techniques for determining Q and discuss the reasons for discrepancies between methods (Badi and Mooney, 1987; Redpath and others, 1982; Jongmans, 1990). The spectral ratio technique is considered the preferred method of Q determination by Badri and Mooney (1987) because it is independent of the source and is more reliable. The spectral ratio method has been exclusively employed in several in situ investigations (McDonal, and others, 1958; Newman and Worthington; 1982). Because it involves the determination of the slope of a least-squares fit, the spectral ratio method is most accurate in the range $5<Q<50$ (Bourbie, and others 1987). Although some claim at least two techniques should be employed to derive Q in situ, when differences arise the spectral ratio technique is generally used as the standard for comparison.

For this study, the manipulations necessary to obtain the compressional wave quality factor, Qp, and the shear wave quality factor, Qs, involved six data sets. To avoid numerous and repetitive illustrations, the shear wave data set obtained on Line 1 in U12p.04 tunnel will be used to illustrate techniques. Illustrations for additional data sets are relegated to the appendix. This also makes for easier comparison of the data between individual sites.

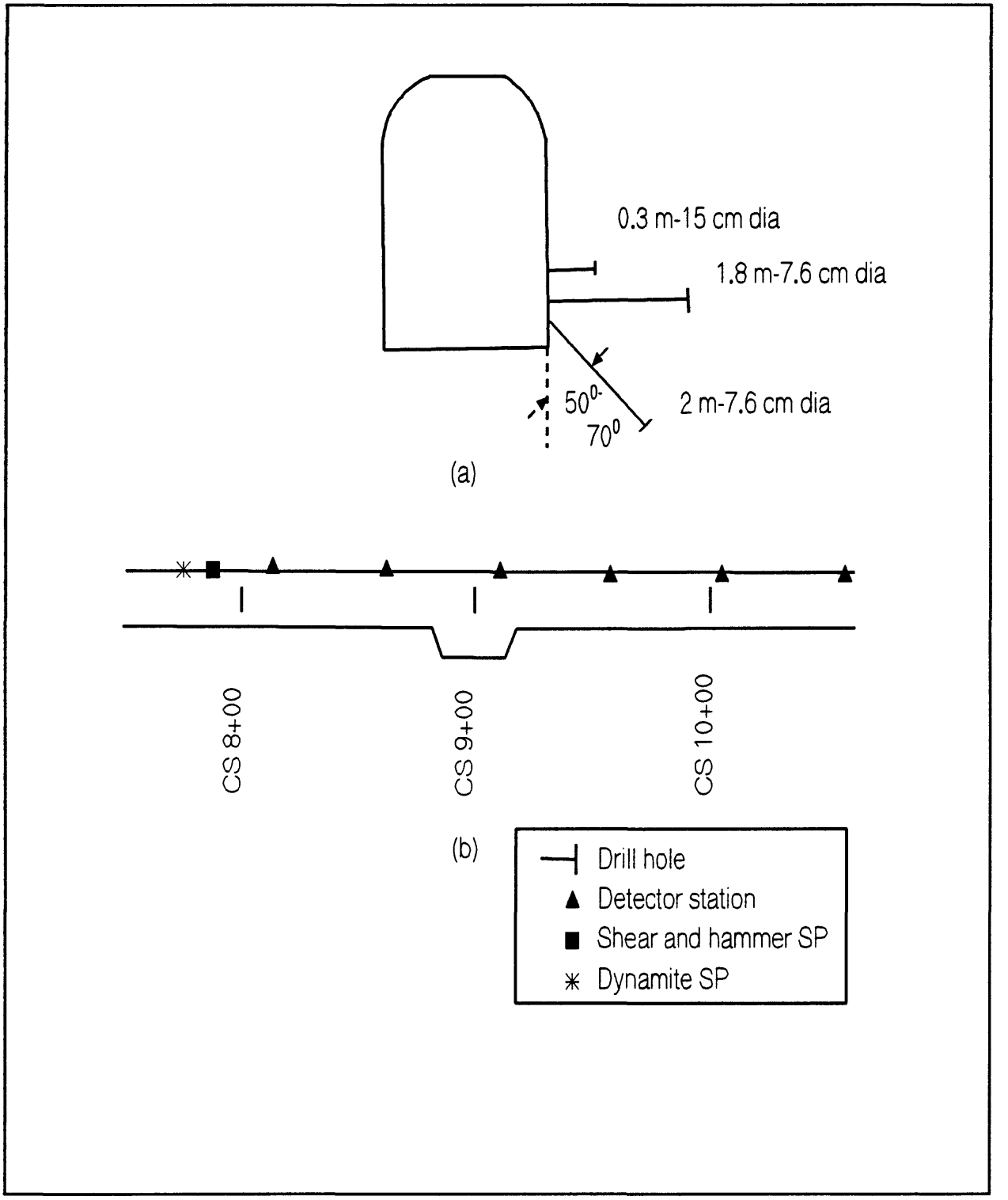

Figure 10.--Layout of seismic line in U12n.05 Utilities drift. a) X-section through typical station, and b) plan view of sensor locations.

Noise was present to various degrees on all data sets, but the first half cycle of the raw data was adequate for picking rise time and amplitude. For spectral analyses, filtering was necessary before the first cycle of each data set was extracted. Tonn (1989) reports that picking the first cycle or a multiple of cycles yields the best definition of Q. Figure 11 shows the raw and filtered shear wave data obtained on Line 1 using the shear sledge source. The shear wave is generally quite clean with this source as is evident on the figure. Compressional wave interference is barely discernible. A 400 Hz low-pass Butterworth filter was applied prior to extracting the first cycle of the shear wave.

In the analyses to follow both raw and filtered data are used where applicable. This is due to the dependence of some techniques of Q determination on the source frequency spectrum. Because filtering artificially changes the source spectrum, comparisons between results obtained from raw and filtered data are informative. **On all plots in this report filtered data points are indicated by open circles.**

Velocity

The shear velocities derived from the data on figure 11 are shown on figure 12. The filtered times of arrival include a time delay due to the filter and thus can be expected to increase the intercept time on the plots. The time-distance plots exhibit no significant breaks which might be associated with refractors in the vicinity of the line, a condition which is typical of the data from all sites.

Spectral Ratio Technique

The spectral ratio method basically entails comparison of the frequency components of the waveform of interest at two ranges, R1 and R2. Thus, from equation 1 the amplitude of the waveform at two detectors is given by,

$$A_1 = \frac{A_0}{R_1} e^{-\frac{\pi f}{QV} R_1} \qquad (4)$$

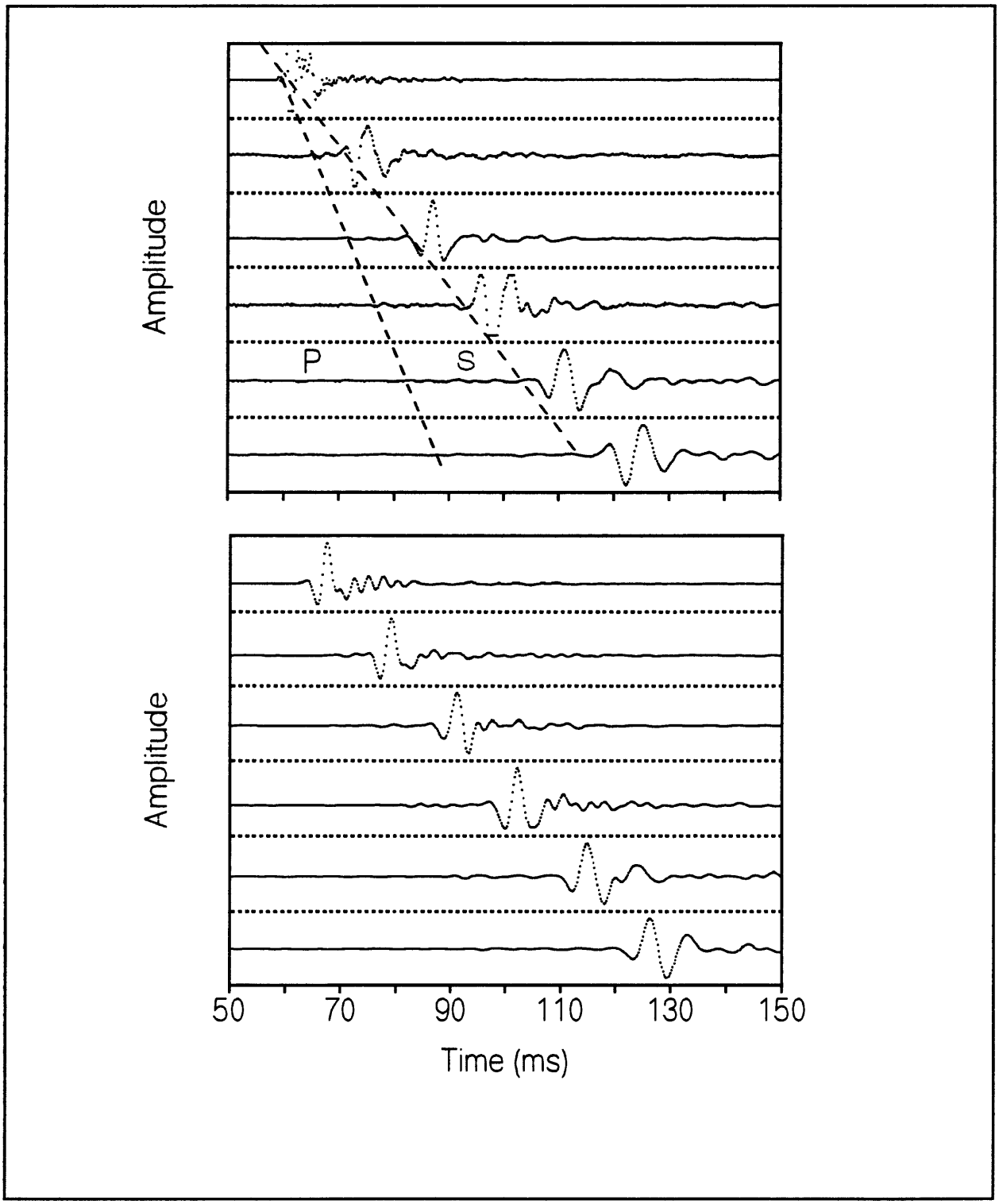

Figure 11.--Unfiltered (top) and 400 Hz filtered (bottom) shear waveforms obtained on Line 1, P04 drift.

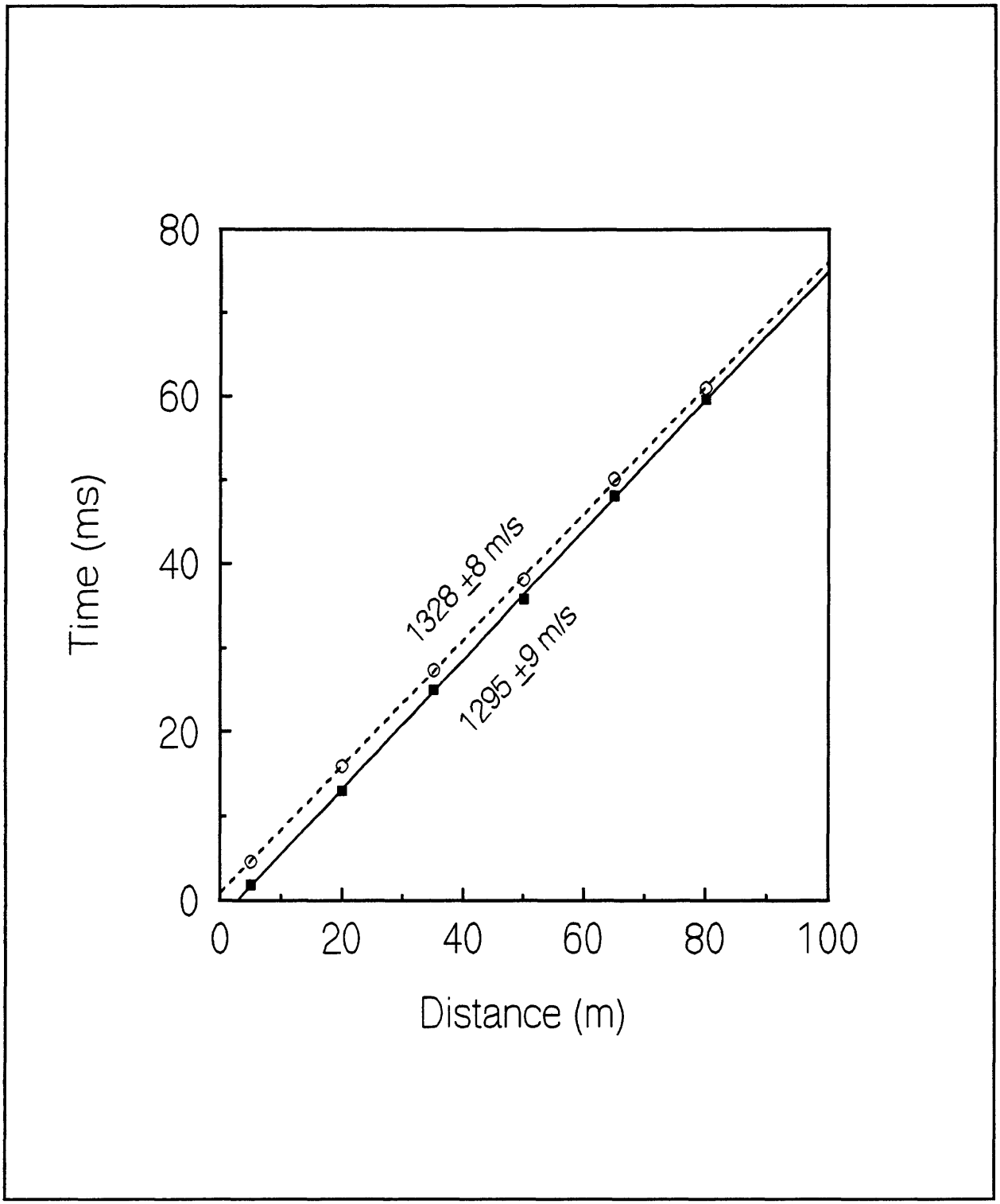

Figure 12.--Shear wave velocities obtained on Line 1, P04 drift.

and,

$$A_2 = \frac{A_0}{R_2} e^{-\frac{\pi f}{QV} R_2} \tag{5}$$

where f is frequency, V is velocity and A_0 is the initial amplitude. Taking the ratio of the amplitudes at the two stations yields,

$$\frac{A_2}{A_1} = \frac{R_2}{R_1} e^{-\frac{\pi f}{QV}(R_2 - R_1)} \tag{6}$$

with the log of both sides providing,

$$Ln\frac{A_2}{A_1} = Ln\frac{R_1}{R_2} - \frac{\pi f}{QV}(R_2 - R_1) \tag{7}$$

Given that the received waveform is a spectrum of frequencies, in the frequency domain equation 4 becomes,

$$Ln\frac{A_2(\omega)}{A_1(\omega)} = Ln\frac{R_1}{R_2} - \frac{\pi \omega}{2QV}(R_2 - R_1) \tag{8}$$

Because all but $A(\omega)$ and ω in (8) are constants, equation 8 may be solved by plotting the log of the amplitude ratios of the frequency components of the seismic pulse against frequency. The slope of this plot is predicted as linear and by a simple calculation yields Q. Under realistic noise and lithologic conditions encountered in field measurements it is desirable to obtain results for several data pairs. Thus, (7) and (8) become

$$Ln\frac{A_n}{A_1} = Ln\frac{R_1}{R_n} - \frac{\pi f}{QV}(R_n - R_1) \tag{9}$$

$$Ln\frac{A_n(\omega)}{A_1(\omega)} = Ln\frac{R_1}{R_n} - \frac{\pi \omega}{2QV}(R_n - R_1) \tag{10}$$

where A_1 is a reference detector, usually taken as that nearest the source. In this investigation, six sensors were employed yielding 5 data pairs when all detector outputs are used.

Dependence of Q on geometric spreading (assumed 1/R in our equations) is not a factor in the spectral ratio method because it is not involved in the slope of the plot of spectral ratio versus frequency, which is derived by operating on equation 10,

$$\frac{\partial}{\partial\omega} = -\frac{\pi}{QV}(R_n - R_1) \qquad (11)$$

The spectral ratio for each station pair is a linear function of frequency, has a negative slope, and for a constant Q exhibits a slope increasing with distance. Equation 12 representing the slope of 10, is again operated on by,

$$\frac{\partial}{\partial R} = -\frac{\pi}{QV} \qquad (12)$$

Thus the slope of a plot of the slopes of 10 versus the distance of each detector pair from the reference detector allows determination of Q by 12. The spectral ratio technique therefore entails a two step process involving the determination of two slopes.

The extracted shear pulse on Line 1 and the associated Fourier transforms for the filtered pulse are shown on figure 13. The number of frequency bins for all data sets ranged from 512 to 1024. The maximum number of data points recorded was 2500 per channel. The minimum number was 1600. Frequency sampling intervals ranged from 5 Hz to 20 Hz, being 5 Hz in this example.

The Fourier transforms depicted on figure 13 qualitatively follow our expectations of attenuation behavior, with the high frequency limb attenuating in a visually systematic manner from the first to the last channel.

Spectral ratios are generally obtained using the station closest to the source as the reference. The distance of the reference station from the source raises the question of near field source terms and their possible influence on the data. In the near field the waveform can be strongly affected by mechanisms unrelated to the attenuation properties of the medium. Thus the source-to-reference detector distance is of some concern. Newman and Worthington (1982) consider a distance of beyond one wavelength as adequate to avoid the problem. Jongmans (1991) analyzed the problem on the basis of rise time considerations and concluded that a 1.2 wavelength offset is required before near field terms may be neglected. Given the offsets and seismic velocities of interest, this indicates frequencies below about 130 Hz for the P wave and 70 Hz for the S wave would be of

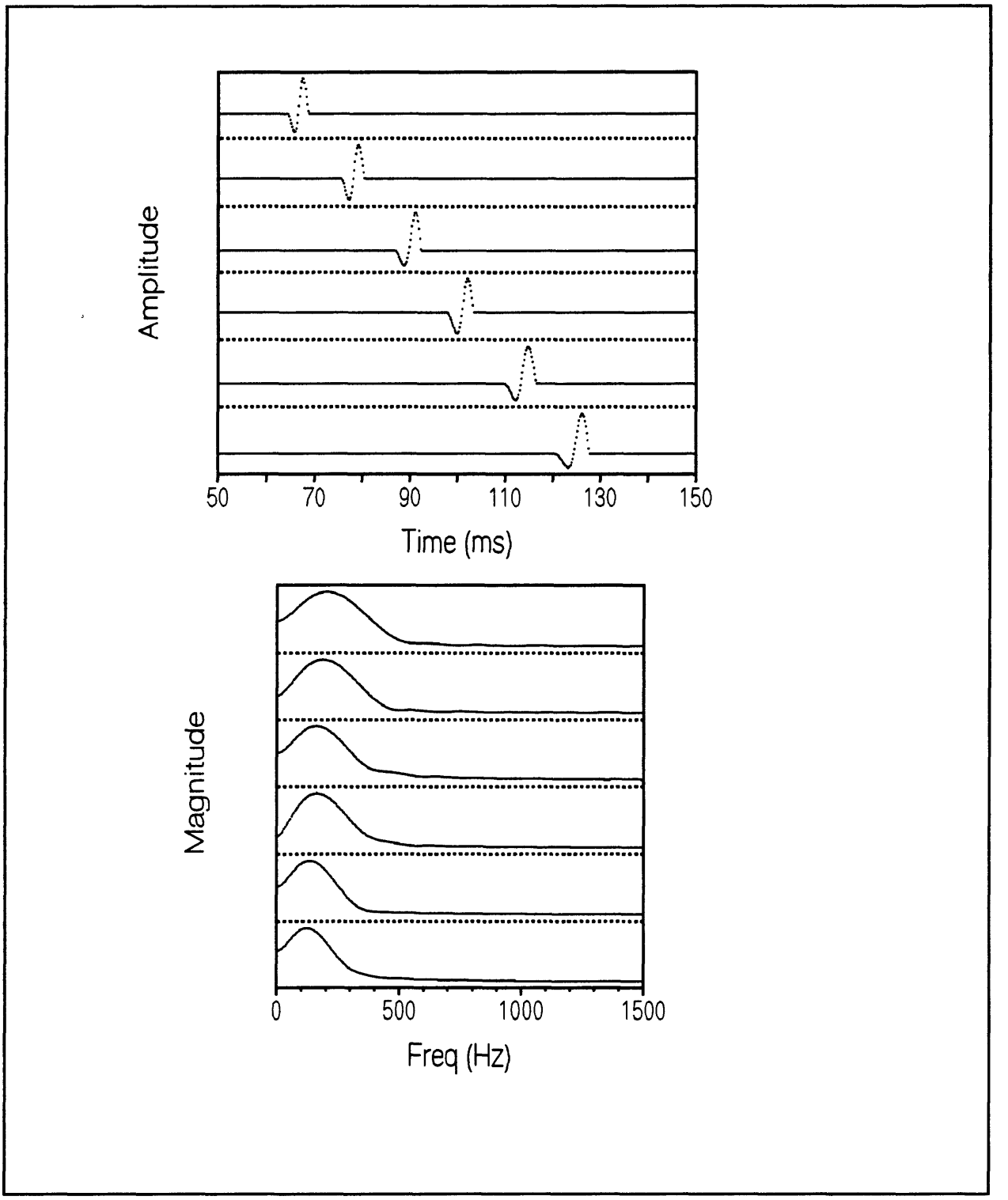

Figure 13.--Extracted shear-wave cycle (top) and FFT (bottom), Line 1, P04 drift.

concern. Bandwidths utilized in this study are generally above these limits, however, in order to provide a check, the spectral ratio data were also plotted using the second detector closest to the source as a reference. The resulting 5 and 4 pair plots are shown on Figure 14 which is the graphical representation of equation 10.

The next step is the selection of a bandwidth over which to determine the slopes used to solve equation 12. The method is obviously somewhat sensitive to the selection process. Because of the negative slope in equation 12, this bandwidth must be selected along the negative slope of spectral curves on figure 14. In this instance the bandwidth 185 to 310 Hz was chosen. Figure 15 is a plot of the slopes obtained within this bandwidth versus distance using the first and second detector as reference stations. The error bars, which are difficult to see on the plot, are one standard deviation of the spectral slopes. The slopes of these two plots are the solutions to equation 11. A value for Qs of 17 is indicated in both analyses.

The attenuation factors obtained at all three sites by the spectral ratio method are listed in table 3, and the associated data plots may be found in the appendix.

The probable error for the spectral ratio technique is given by

$$S_Q = \left(\left(-\frac{Q}{m} Sm \right)^2 + \left(-\frac{Q}{V} Sv \right)^2 \right)^{1/2} \qquad (13)$$

where m and V are the slope of the spectral ratio and velocity, respectively, with errors of Sm and Sv. Many authors report a value for Q and an associated error without reference to the method of error calculation. Frequently it appears to be the error associated with the slope. The error estimated in our data are the probable errors extracted by the propagation of error method.[4]

With the exception of Qs derived in N tunnel the results are quite consistent indicating that near-field effects are probably negligible. The value of 69 derived for Qs at N tunnel is unreliable because the slope is based on only three data points.

---

[4]It is recognized that for the spectral ratio technique the error does not take into account the sensitivity involved in the selection of the bandwidth nor the error in the slope determined from equation 12. The one standard error bars for these slopes are generally small, being barely discernible on figure 14.

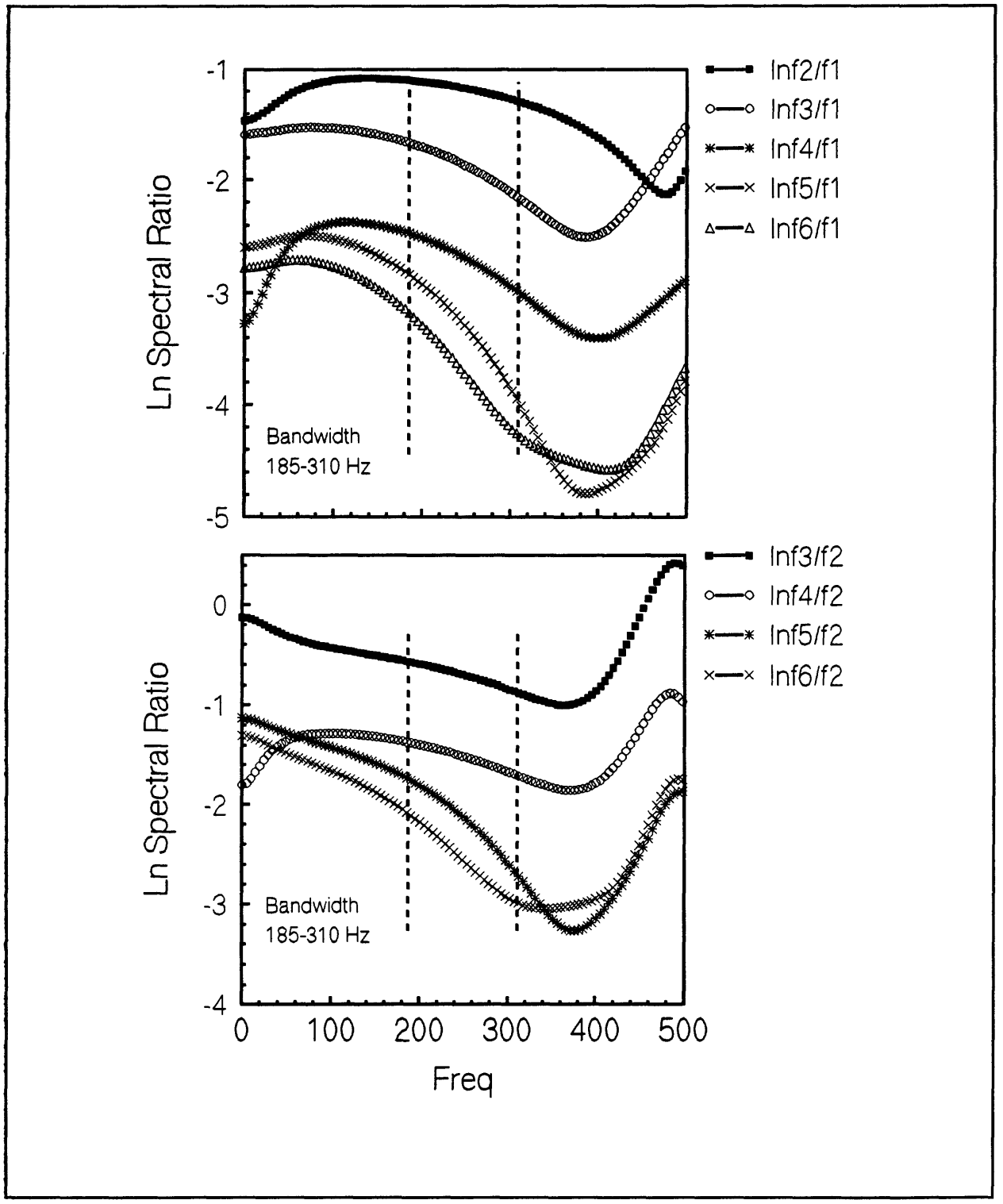

Figure 14.--Spectral ratios for extracted shear-wave cycle using 1st detector (top) and 2nd detector (bottom) as reference. Line 1, P04 drift. Slopes extracted over 185-310 Hz bandwidth. Shear wave, Line 1, P04 drift.

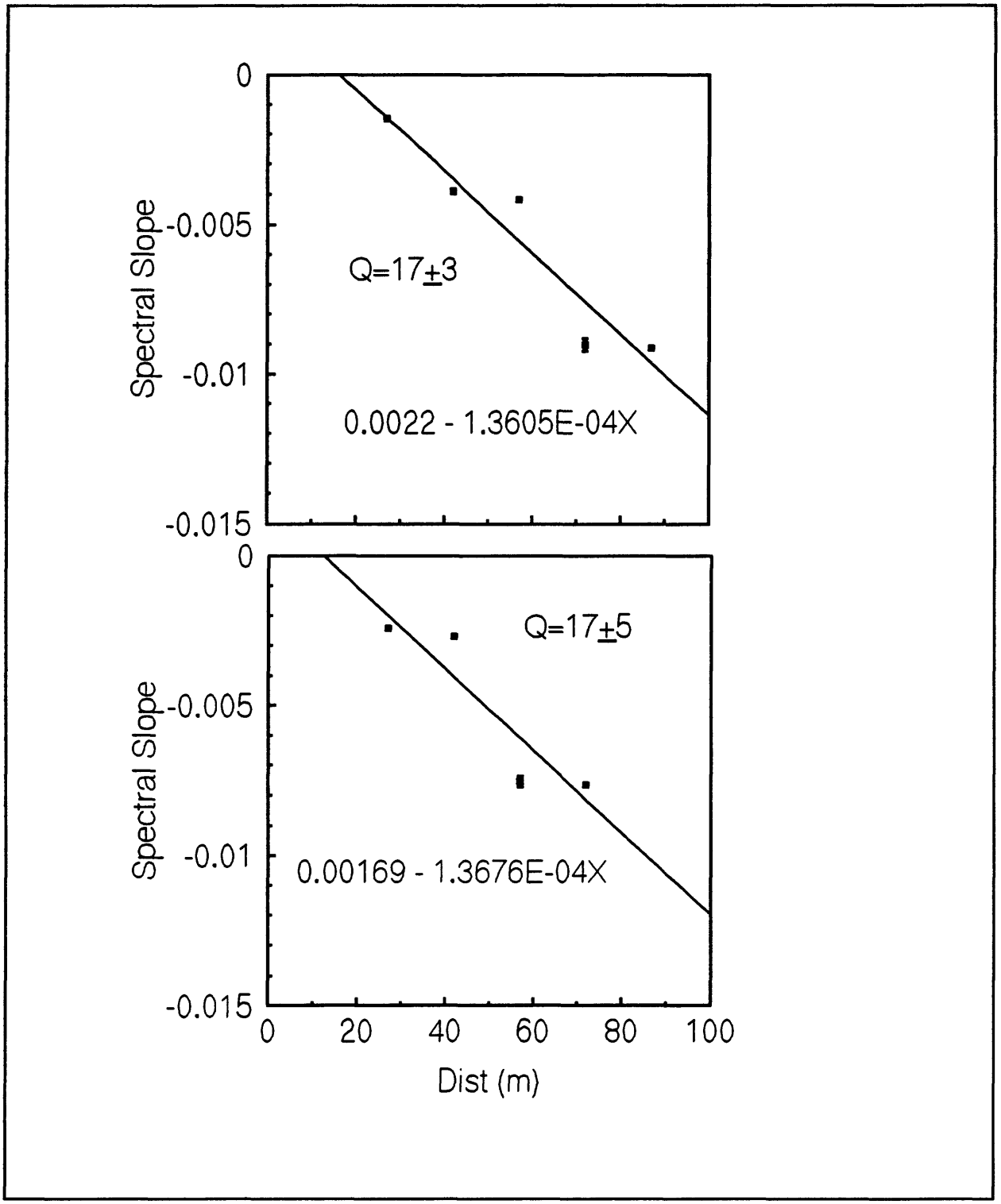

Figure 15.--Spectral slopes versus distance using 1st detector (top) and 2nd detector (bottom) as references. Shear wave, Line 1, P04 drift.

Table 3.--Values of attenuation factor (Q) obtained from spectral ratio technique.[1]

Location	Q
Line1 Qs	17±3/17±5
Line2 Qs	22±3/23±4
NQs	36±11/69±43[2]
Line1 Qp	18±2/17±5
Line2 Qp	--
NQp	24±4/19±6[2]

[1]First figure refers to detector nearest source as reference; second uses second detector.
[2]Data at far detector not used in analysis.
-- No data

Rise Time

The loss of the high frequency components of the seismic pulse with distance is also a measure of Q, either as observed in increasing pulse width or decreasing rise time. The utility of this as a measure of Q was recognized by Gladwin and Stacy (1974) who described the behavior of this change in pulse shape as

$$t = t_0 + \frac{C}{Q} T \tag{14}$$

where t is the rise time, t_0 is the rise time of the initial pulse, T is the arrival time, and C is a constant. Thus the slope resulting from a simple plot of rise time versus time of arrival at each detector is adequate to determine Q if the constant C is known. Blair and Spathis (1984) state that any reasonably defined measure of rise time will follow the relationship of (14) and pulse broadening using this technique has been defined in a number of ways. Figure 16 depicts the three measurements defining pulse broadening which were investigated in this study. The measurement identified by T_a and initially used by Gladwin and Stacey is that most often used to derive the rise time from the seismic pulse. This method is simply derived because it is maximum slope divided by maximum amplitude or

$$A_{max} \Big/ \frac{\partial A}{\partial t_{max}} \tag{15}$$

The result can be seen to be sensitive to any amplitude or zero baseline noise. Gladwin and Stacey estimated C to be 0.53 based on field measurements using this definition (Gladwin and Stacey, 1974; Stacey and others, 1975). Kjartansson (1979), in providing a theoretical basis for the technique, derived a value of C=0.485 for an impulse displacement source and 0.298 for use with a velocity detector. Kjartansson also derived a theoretical value of C=1 if the pulse half width is used as the broadening measure, and geophones are employed as detectors. Blair and Spathis

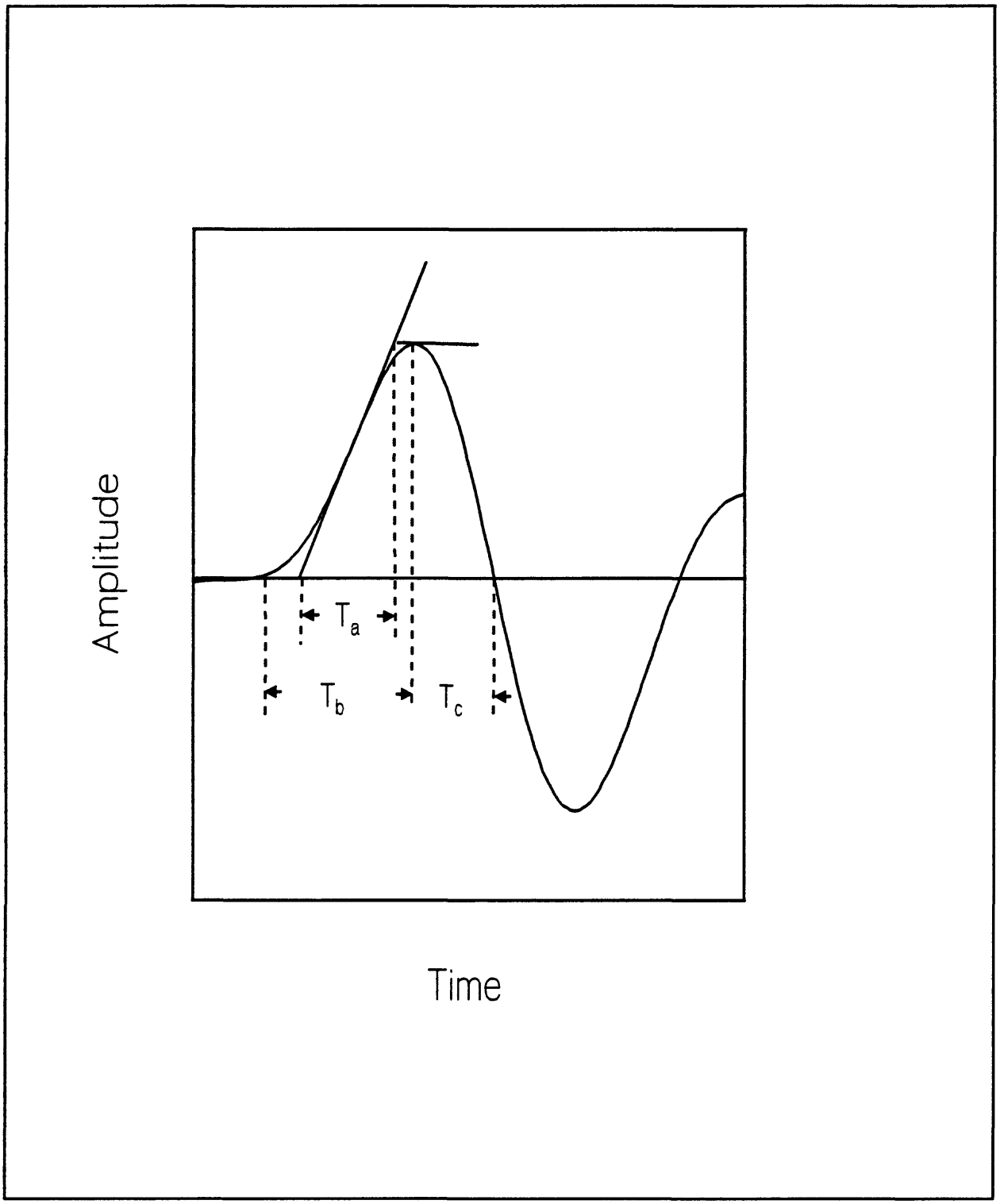

Figure 16.--Three definitions of pulse broadening used in attenuation studies.

(1982) derived a theoretical value of 0.217 for accelerometers. However, many authors still seem to use C=0.5 arbitrarily (Wright and Hoy, 1981; McKenzie and others, 1982). Badri and Mooney (1987) used a value of 0.5 with what was essentially the first quarter as well as the half period of the initial pulse. Hatherly (1986) utilizes a value of C equal to 0.3 in geophone surveys where the value of Q is estimated from refracted arrivals. He uses a definition of rise time which is approximately the quarter period. A further difficulty lies in the use of a constant value of C regardless of the magnitude of the derived Q. Kjartansson clearly restricts the applicability of a constant value of C to values of Q greater than about 20.

Although there is some uncertainty as to the theoretical value of C applicable to a given source-receiver type and the measurement used to define pulse broadening, the choice is academic because of the demonstrated dependence of C on the seismic source. This was shown experimentally by Blair and Spathis (1982,1984) and confirmed theoretically for different source functions by Stewart (1984) and Liu (1988). Although some of these theoretical source functions appear somewhat esoteric, they indicate that the value of C may be greater or less than that obtained by a unit impulse depending on the nature of the source. Laboratory studies on core by Tarif and Bourbie (1987) also demonstrate the source dependence of C. In our study the values T_a, T_b, and T_c were all examined. For shear wave data there is often added uncertainty as to the exact onset of the shear arrival, with the possibility that in some instances a weak precursor defining onset may have been lost in noise. In the case of the shear wave, the pulse width of the central lobe may be more useful.

The rise time technique is sensitive to signal-to-noise ratio but has the advantage that it is not affected by geometric spreading and does not require the use of a frequency spectrum. Its main advantage is that, because it involves only the initial quarter cycle of the waveform, effects on the full pulse due to interference from later arrivals, a problem in many in situ investigations, is minimized.

Figure 17 depicts plots of rise time versus arrival time obtained for the filtered and unfiltered data on Line 1 in P tunnel. These data were derived using T_a as the definition of rise time. Filter delay is evident on the filtered data, however, in many cases the plot of the raw data does not pass through the origin as might be expected if the source function were a true impulse.[5] A difference in slope between the two plots follows from the

---

[5]Dependence of rise time on source spectrum is intuitive. What variations in C seem to suggest is that the spectrums of small dynamite sources can significantly differ in some, if not most, environments. Comparative studies demonstrating this were not found in the literature.

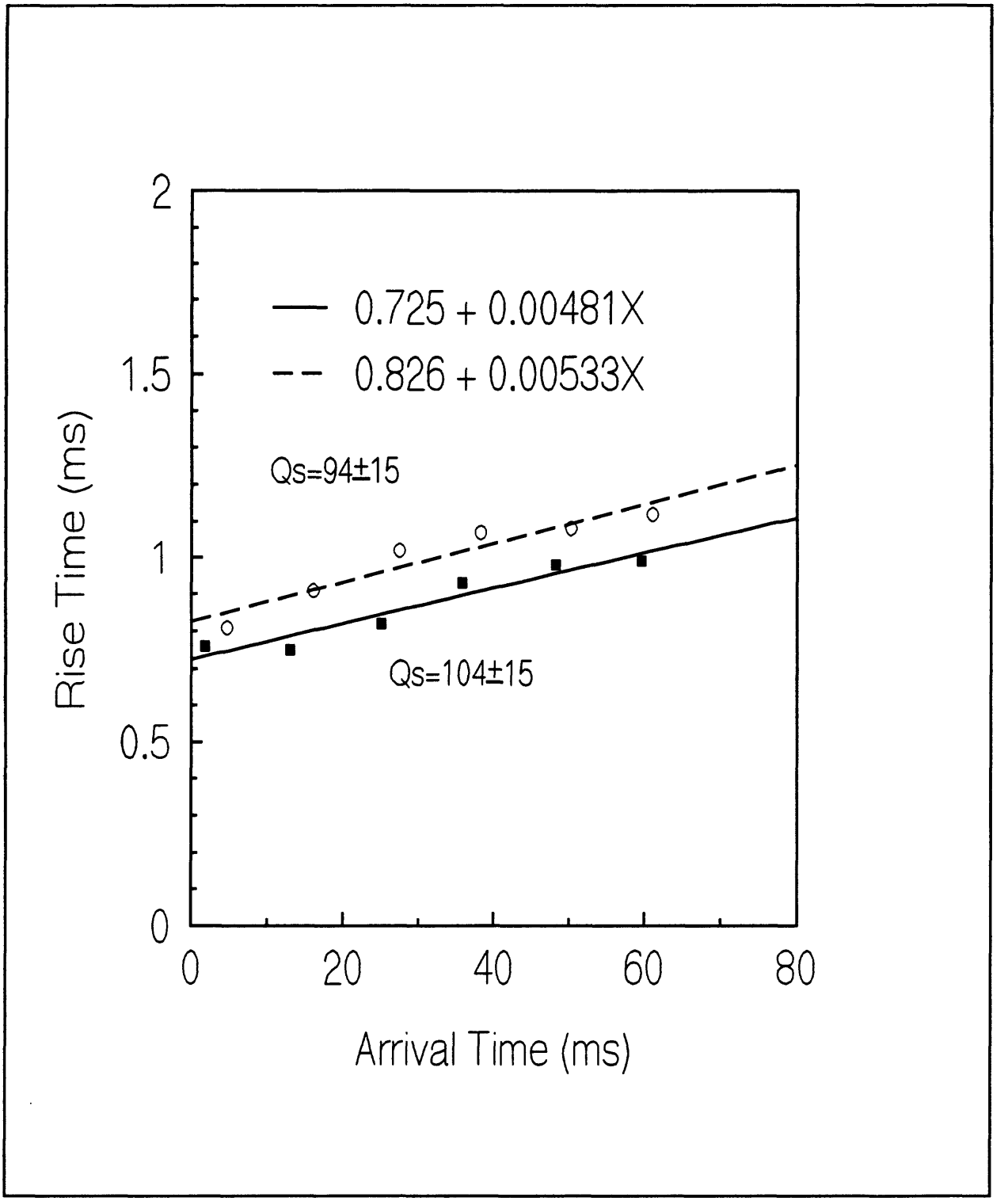

Figure 17.--Rise time versus arrival time for shear wave obtained on Line 1, P04 drift.

observed dependence of the constant C in equation 15 on the source spectrum. Although there is considerably greater scatter in the raw data, the improvement in fit for the filtered data is not observed at all sites. However, as expected, a greater slope is observed for the raw data. Values of Q derived from the rise time T_a and assuming a value of C of 0.5 are listed in table 4.

Table 4.--Values of attenuation factor(Q) obtained from rise time data.

Location	Raw Data	Filtered data
Line1 Qs	104±15	94±15
Line2 Qs	57±25	32±8
N Qs	*	*
Line1 Qp	23±2	16±4
Line2 Qp	34±5	No data
N Qp	9±2	*

* No correlation (R <0.25). All others R≥0.9

The probable error in Q is obtained from the slope of equation 15 as,

$$Sq=\frac{Q}{m}Sm \qquad (16)$$

where m is the slope of the rise time plot with associated error Sm.

Values of Q derived from the other definitions of rise time depicted on figure 16 are listed in table A1 in the appendix. For comparison, plots of rise time (T_b) versus arrival time are also listed in the appendix for each site. T_c in some instances is affected by interference effects on the late portion of the waveform. The three data sets are listed to compare the effect on Q of the choice of the pulse broadening parameter. Any choice seems to generally provide a good linear fit, however, aside from realizing that T_b is sensitive to gain and that filtering is, in effect, changing the source, uncertainty exists as to the applicability of these data to providing a realistic value of Q.

Many investigators have reported that Q derived from using T_a is highly overestimated (Badri and Mooney, 1987; Redpath and others, 1982). Overestimation of Q derived from rise times as compared to the spectral ratio technique is also reported by Jongmans when using C=0.285 with geophone detectors (Jongmans, 1990). This appears to be in agreement with this study. The rise time technique is also sensitive to noise. Plots of field measurements of rise time versus arrival time can often be quite poor, with statistically meaningless correlations (see, for

example, some of the data of Wright and Hoy, 1981; Hatherly, 1986). For high or low values of Q the technique is considered superior to the spectral ratio method because of the sensitivity of the spectral slopes in these ranges. The uncertainty in the value of C applicable to the source function has led many to not rely on the rise time method with a fixed value of C. Hatherly reports C=0.3 as applicable to values of Q derived from several seismic refraction surveys, although his basis for this is not clear. Tarif and Bourbie (1987), in comparing attenuation derived from samples in the laboratory, concluded that a) the rise time method is permissive of the measurement of strong attenuation (Q<5) whereas the spectral ratio method is not, b) the rise time method is more sensitive to noise than the spectral ratio technique, and c) both rise time and spectral ratio techniques yield poor precision where Q>100. They reiterate the conclusions of other investigators regarding the difficulty in determining C.

For our results the filtered data should provide Q values lower than the raw data strictly because of larger slopes obtained. This is generally the case except for the N tunnel site. The absence of correlation for some of the N tunnel data may be due to either noise or interference effects. Filtering of the data acquired at this site involved the lowest cutoff frequency and the "raw" data were also obtained with a 1kHz analog filter in the line to reduce noise. There is a similarity in derived Q for some data regardless of filtering, which is not strictly restricted to the sites in which the filtered data had the highest cutoff frequencies. The results using Tc as the definition of pulse broadening yield similar Q values in several instances. Stewart (1984) demonstrates for some idealized pulses that the slope of the plot of fall time (which Tc may approximate) versus arrival time is less variable than rise time with source variation. However, fall time might be difficult to define for realistic waveforms. Badri and Mooney (1987) also found Q dependent on the definition of pulse broadening using a constant C.

Finally, notice should be taken of the limitations of geophones in recording raw rise times for the higher frequency spectrums because of the inherent bandwidth limitations of these devices. If rise time techniques are to be employed with geophones, these limitations should be investigated.

Time domain amplitudes

Equation 1 or 9 may be used to obtain Q in the time domain if a reasonable average value of frequency is known. This approach has been used by some investigators utilizing the dominant frequency on the seismic record. The geometric spreading exponent (normally assumed unity) becomes important for the time domain case because amplitudes must be multiplied by distance from the source before plotting. Thus equation 9 becomes

$$Ln(A_n R_n) = Ln(A_1 R_1) - \frac{\pi f}{QV}(R_n - R_1) = C - \frac{\pi f}{QV} R_n \qquad (17)$$

where C is a constant. The slope of the plot of the left side of (17) versus distance yields the time-domain derivation of Q. One plots the left side of (17) against distance from the reference detector to obtain the slope necessary to derive Q. Some prefer to plot an amplitude ratio similar to the spectral ratio technique, using the amplitude at the detector nearest the source as the reference. This eliminates the intercept C in (17) and the resulting plot should be linear through the origin if geometric spreading follows 1/R (or whatever dependence in R is assumed). The plot obtained using the ratio technique is shown on figure 18. Plots derived employing both techniques are presented in the appendix.

The time domain technique requires a representative value of frequency, which if the method is to have utility, should obviously be derived from time domain data. The general approach is to select the dominant frequency of the first cycle of the waveform. Hatherly (1986) claims subsequent zero crossings are a sufficient approximation to the wave period. Tb was assumed the quarter period in deriving the dominant frequency to obtain the Q shown on all plots in this report. Values of Q for both the raw and filtered data are listed in table 5. Results obtained using Ta, Tb, and Tc as measures of period and the two methods of reduction are shown in table A2 in the appendix.

Table 5.--Values of attenuation factor (Q) derived by time-domain amplitude-ratio method.

Location	Raw Data	Filtered Data
Line1 Qs	18±7	13±4
Line2 Qs	9±6	8±3
N Qs	10±5	11±5
Line1 Qp	5±4	5±2
Line2 Qp	6±3	No data
N Qp	4±4	2±1

For the time domain case, Q is given by

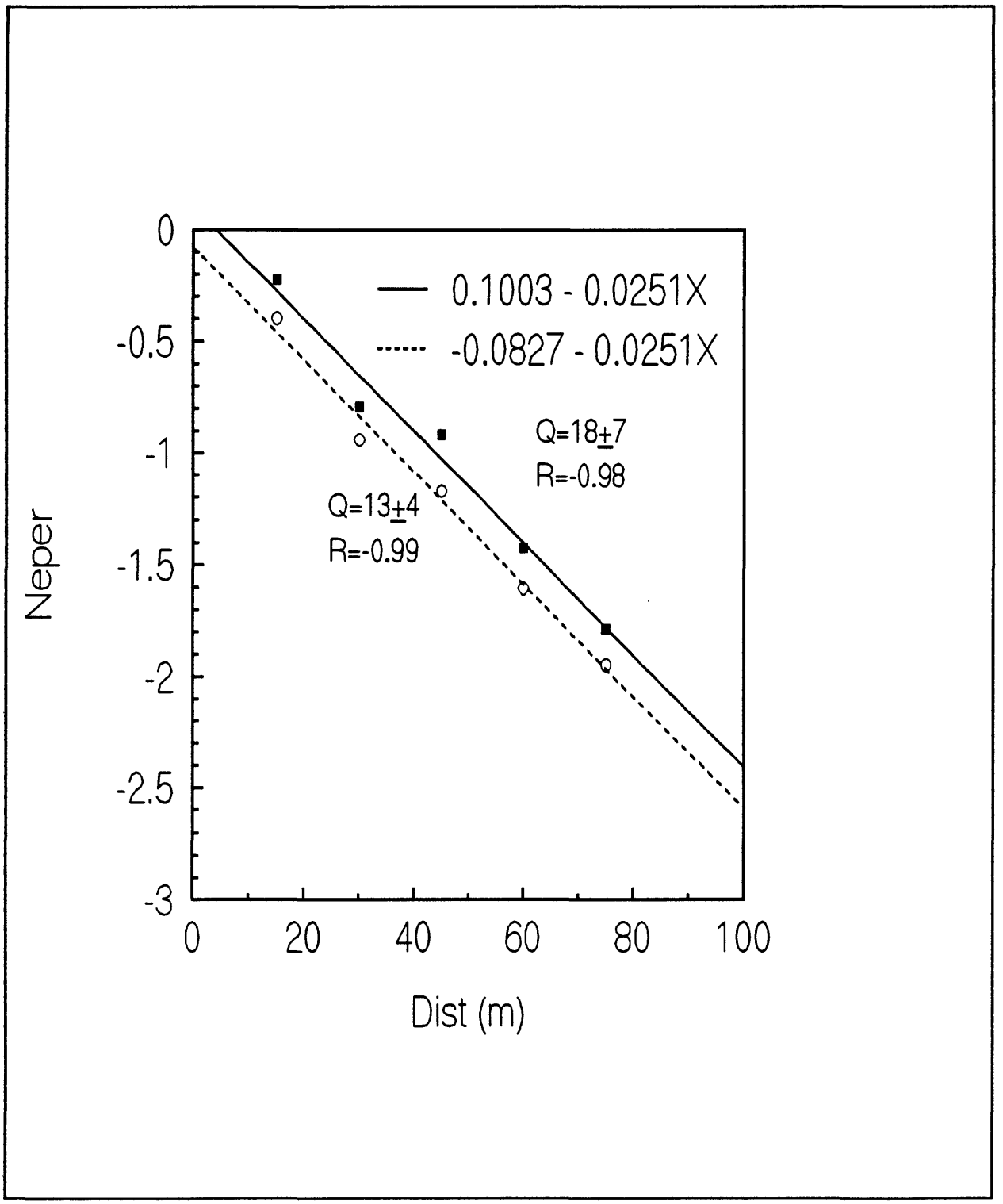

Figure 18.--Plot of time-domain amplitude-ratio versus distance. Shear wave, Line 1, P tunnel.

$$Q=\frac{\pi}{mVT} \tag{18}$$

where m is the slope of the amplitude versus distance plot, V is the velocity, and T is the dominant period observed on the record. The associated errors of these variables (Sm, Sv, St) lead to the probable error in Q,

$$Sq=\left(\left(-\frac{Q}{m}Sm\right)^2+\left(-\frac{Q}{T}St\right)^2+\left(-\frac{Q}{V}Sv\right)^2\right)^{1/2} \tag{19}$$

Unlike the spectral ratio method and the rise-time method, the time-domain amplitude technique appears to consistently yield lower values for Qp than for Qs for our data. The choice of a single frequency to derive Q via this technique involves an average of the dominant frequency at each detector, which can have a considerable standard deviation. Newman and Worthington (1982) report values of Q derived from the time-domain technique as equivalent to those obtained by spectral ratio. However, they claim a more precise value of Q is obtained from the spectral ratio method. Conversely, Badri and Mooney (1987) report inordinately high values of Q obtained from time domain measurements as opposed to the spectral ratio technique. Anderson found the technique gave results equivalent to other methods in a backfill material exhibiting Q near 8 (K. R. Anderson, Air Force Weapons Lab, written commun; 1990). For our data the choice of period based upon average T_a, T_b, or T_c effects the results in only a few cases. Reducing the data using amplitude versus distance yields slightly more consistent Q values than does using amplitude ratios.

Propagation Technique

The uncertainty in the proper value of C to use with the rise time technique prompted Blair and Spathis (1982,1984) to utilize the spectrum near the source and mathematically propagate the source spectrum to match rise times observed at other detectors by varying Q. This method is considered particularly applicable in cases of interference by other events on later parts of the pulse. The method requires only the full spectrum near the source and the rise time portion of the pulse at the more distant stations where interference from reflection and refraction is often most dominant. A suitable transfer function is required. Blair and Spathis utilized the attenuation model of Kajartansson (1979) in propagating the source spectrum. The Kjartansson propagation equation is

$$B(\omega) = \exp-\{(\frac{2x\pi f_0}{c_0}\frac{f}{f_0}^{1-\gamma})\,[\tan(\frac{\pi\gamma}{2}) + isgn(f)]\} \qquad (20)$$

where

$$\gamma = \frac{1}{\pi}\tan^{-1}(\frac{1}{Q}) \approx \frac{1}{\pi Q} \qquad (21)$$

and f, c, and x are frequency, velocity, and distance. f_0 and c_0 are a reference frequency and velocity, often taken as the dominant frequency and travel time velocity.

The calculation of the propagation of the Fourier spectrum is often facilitated by the use of the real and imaginary parts of (20). Thus letting

$$A(x,f) = \exp-\{\frac{2x\pi f_0}{c_0}\frac{f}{f_0}^{1-\gamma}\tan\frac{\pi\gamma}{2}\} \qquad (22)$$

$$B(x,f) = \{\frac{2x\pi f_0}{c_0}\frac{f}{f_0}^{1-\gamma}\} \qquad (23)$$

then

$$ImB(\omega) = A\sin(Bsgn(f)) \qquad (24)$$

and

$$ReB(w) = A\cos B \qquad (25)$$

Blair and Spathis (1982, 1984) in applying the propagation technique to field data found that the attenuation transfer functions of Azimi, and others (1968) and Strick (1970) yielded values for Q similar to those obtained with the Kjartansson transfer function.

Because of the poor rise time correlation for the N tunnel data a determination of Q by this technique was not attempted. Jongmans (1990) reports that this technique overestimates Q compared to the spectral ratio method. Jongmans further found that values of C for the rise time technique ranging from 0.11 to 0.2 were

required to match Q determined from the propagation technique. Blair and Spathis (1982), in their paper demonstrating the source dependency of the constant C used in the rise time technique, derived a value of C=0.15 (accelerometer detectors) based on the propagation technique, a value which they state cannot be derived from any impulse source theory. Tarif and Bourbie (1987) in comparing the propagation technique with the spectral ratio method for core measurements, found the value of Q comparable within experimental error.

The environment of the Rainier Mesa tunnels and the layouts used in this investigation somewhat qualifies the usual justification for employing the propagation technique in deriving Qp. Dynamite sources in the tunnels frequently produce strong SV components. Figure A29 in the appendix illustrates one example. In such cases the near source spectrum is the one of concern with respect to interference. The necessity of a clean P-wave pulse near the source dictates the need for sufficiently long offsets to allow separation of the P- and S-wave arrivals. This requirement probably overrides any concern about offset being large enough to exclude near source effects in the reference pulse, but could conceivably place the reference detector in a region where interference effects the reference pulse.

Source spectra

Figure 19 is a reproduction of source spectra obtained from the full record by dynamite and accelerometer and by shear sledge and geophone. Although these data are not an exhaustive examination of the spectra generated by these sources in the Rainier Mesa tunnel environment, they suggest that spectra at P tunnel sites may be richer in higher frequency components due to some coupling phenomena inherent in the tuff at that location. This could be part of the explanation for the observed requirement for noticeably larger explosive charges at P tunnel when performing refraction surveys than has been the case in other tunnels in Rainier Mesa.

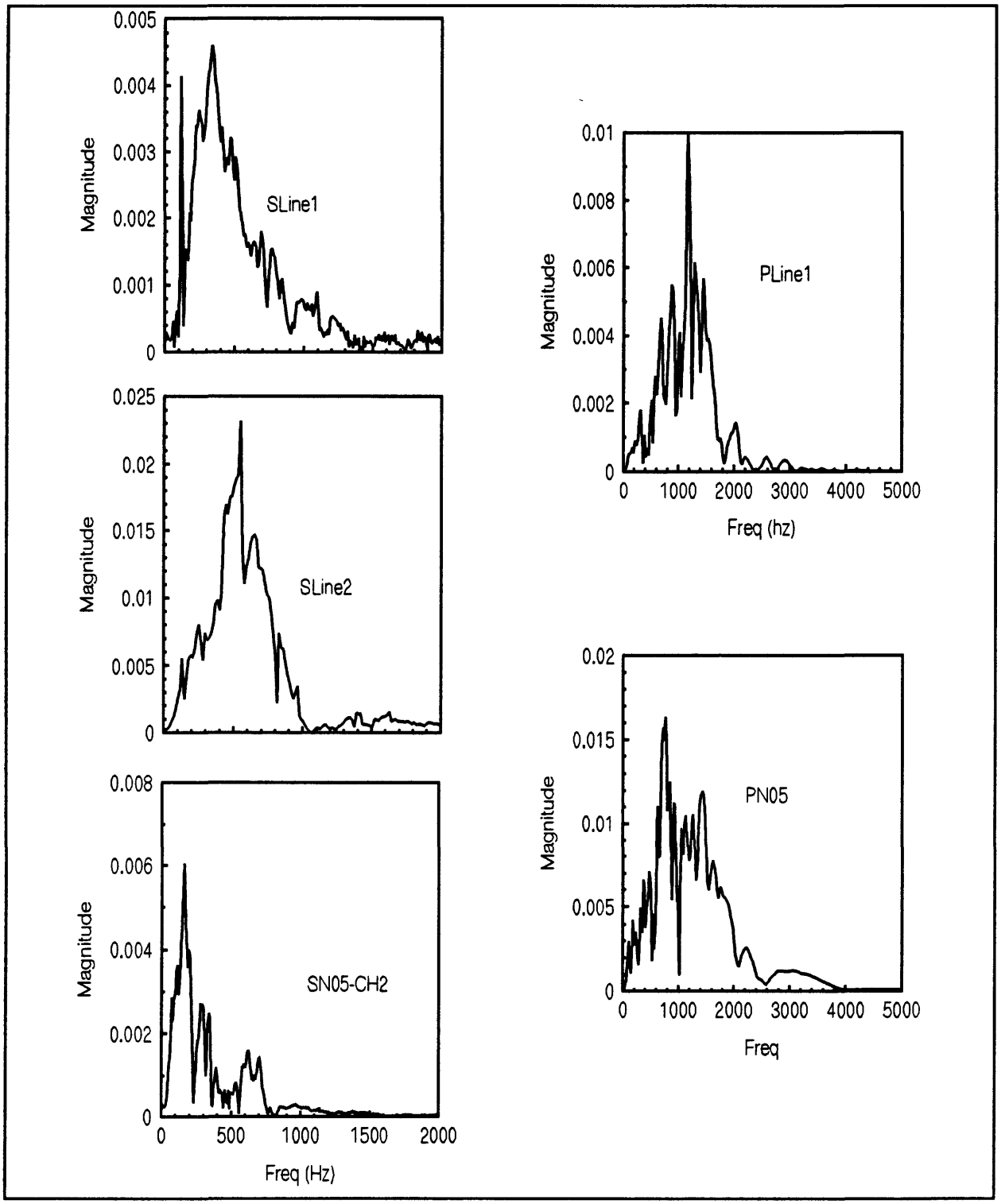

Figure 19.--Frequency spectra obtained at P and N tunnel sites. All S wave data were obtained with shear sledge and L40A geophones. P wave data were obtained with dynamite and accelerometers.

SUMMARY AND CONCLUSIONS

It is apparent from the laboratory studies of other investigators that attenuation is considerably more sensitive to rock properties which affect seismic properties than is P- and S-wave velocity.[6] Attenuation may also be considered a good diagnostic of changes in the bulk parameters which affect shock wave attenuation--strength and air voids, particularly the latter. On the basis of the studies undertaken in P and N tunnels it is also evident that the in situ derivation of Q is relatively straightforward, that is, relatively well behaved plots of the spectral ratio, the rise time versus arrival time, and time domain amplitude versus distance are generally obtained. Comparison of the results obtained by the three methods are shown on figure 20. What is not observed is any equality in the derived values of Q between the three techniques nor any consistency in the trend of comparative values of Q between the three sites investigated. Thus the measurement is not as straightforward as velocity, assuming that interference or scattering are not contaminating the data, possibly a large assumption. Data from numerous records in N tunnel did not consistently provide a reasonable interpretation. The high cutoff filtering required, possibly because of construction features present at that site, lead to the suspicion of interference in the primary pulse. Cultural effects are also suggested as responsible for the obvious contamination of the P wave data on Line 2 in P tunnel. Thus we are faced with the determination of the proper value of Q to use to answer the main question driving this study--what is the difference, if any, in seismic attenuation at P and N tunnels? In answering this question we are faced with the possibility that, in following the lead of other investigators in examining alternates to the spectral ratio method, one becomes discouraged with the overall technique because of little agreement between methods. This dilemma faced Badri and Mooney (1987) when they, like most investigators, concluded that the standard in such cases is the spectral ratio method.

The spectral ratio is not dependent on the source spectrum nor upon artificial operations on the data such as filtering. It is not affected by amplitude, coupling, or gain variations if the true frequency spectrum of the signal is captured. The Q values derived in this study are within the optimum range of applicability of the method. The results of the spectral ratio method (table 3) suggest that the tuff at N tunnel exhibits less attenuation than at P tunnel for both P and S waves. Within the P tunnel complex itself, Line 1 within the U12p.02 equivalent

---

[6]The lack of sensitivity of shear wave velocity to saturation, however, may obviously be a more desirable diagnostic than a measure of attenuation in some applications in Rainier Mesa.

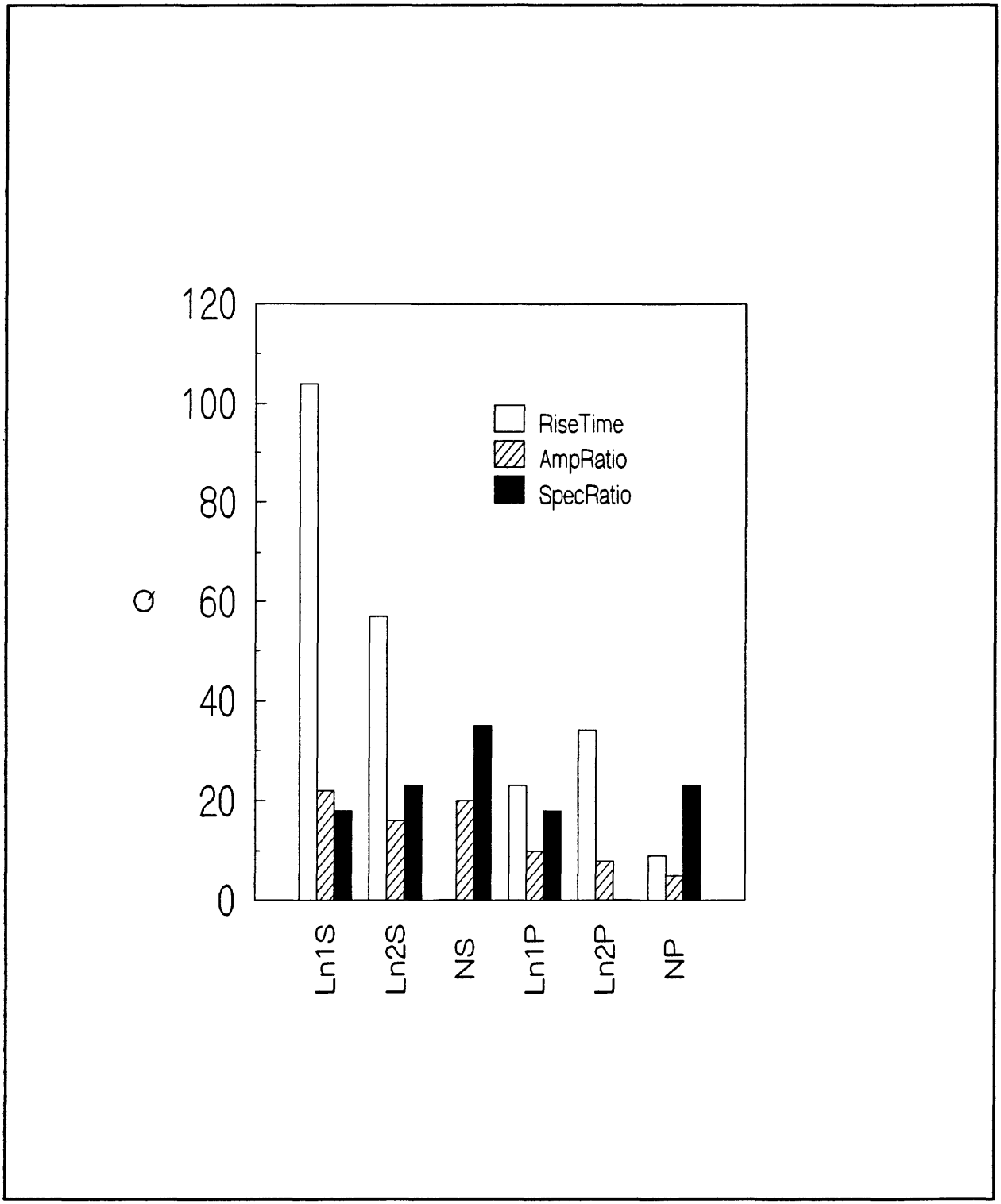

Figure 20.--Comparison of Qp and Qs obtained by three techniques on Lines 1 and 2 in P tunnel and at N tunnel site. Rise time data derived using Ta as definition of pulse broadening.

lithologic setting, exhibits a slightly greater attenuation for Qs than does the U12p.04 stemming region. Because of interference effects on the P wave on Line 2, no comparison between Qp at P tunnel sites is available.

The rise time method is flawed because of the source dependence of C. However, its great simplicity and generally impressive linearity in plotting results in many arbitrarily applying it e.g., Murphy and Rosenbaum (1989). Filtering of the data, as was required in this study obviously changes the rise time, however, Q derived from unfiltered data is also of dubious utility. In the presence of strong noise Tarif and Bourbie (1987) found the spectral ratio reliable as opposed to the rise time technique. Stacking might be more liberally applied than was case in our surveys to increase signal-to-noise in some instances. Two techniques occur to us which might render the technique of useful when comparative values at two or more sites are of interest. One might attempt filtering the data to obtain similar intercepts on the rise time versus arrival time plot, or apply spectral shaping to obtain source pulses (nearest detector) which are similar and propagate the shaping through the spectrums at all detectors. The difference in rise time slopes might then be a direct measure of differences in Q. Blair and Spathis (1982) correctly point out that intercepts on the rise time plot can be the same but spectrums can significantly differ in lower frequency components which do not affect the rise time measurement. Thus, the limits on a strictly time-domain filtering approach need to be investigated. Spectral shaping, of course, involves the frequency domain, and it is arguable whether any advantage, other than redundancy, is obtained over the use of the spectral ratio technique unless Q is very high or low. In some cases it may provide insights into the efficacy of the spectral method. Neither of these approaches were investigated in this study. In our view the rise time technique as a stand alone method remains a method yet to be perfected.

The time-domain amplitude-ratio technique is somewhat more difficult to dismiss. The values obtained seem to be consistent at any particular site. Amplitudes were single peak amplitudes, peak-to-peak values were not examined. Badri and Mooney (1987) found discrepancies between time-domain amplitude-ratio values of Q (higher) than those obtained by spectral ratio. They regard the method as less reliable than that of spectral ratios because of the inherent assumption of monochromatic frequency used in the data reduction, an assumption basically at variance with the reality of seismic wave propagation and attenuation. The variation of fundamental frequency over the short spread lengths employed in our investigations is equivalent to the variations in rise times, which average about a factor of four, ranging from 2 to 9. The justification for using an average frequency value under these conditions is subject to question. This, coupled with uncertainties in the definition of fundamental frequency inherent in describing an asymmetric waveform render the

technique suspect. Tonn (1989), in a theoretical study of seven methods of determining Q, found that the amplitude decay technique provided the least reliable technique for deriving Q, failing in almost all cases. He also found the rise time technique almost as poor. It should be noted, however, that he chose Q values for his hypothetical layers generally in excess of 100.

A frequency domain approach might be applied to the amplitude decay technique in cases where source spectrums are not significantly different. Spectral shaping would allow a direct comparison between time domain slopes and Q would compare nearly directly as the seismic velocities. The same caveats apply to this approach as with the rise time method.

The measurements of Q in the Rainier Mesa tunnels described in this report are, on reflection, considered something of a feasibility study. The technique can obviously be complex and the data subject to interference effects which are difficult to recognize. Therefore, the applicability of the technique requires a greater data base within Rainier Mesa than just the three sites involved in this study, particularly given our concerns about the data at the N tunnel site. The following are some guidelines for future application.

(1) Shear wave pulses (more specifically SV) are generally clean and strongly defined using the mechanical sources employed in this study. SH type shear waves should be as cleanly generated and included in future studies. Defining the onset of rise time by standard techniques (Ta) is less certain for shear waves than the measurement of the pulse width for these wave types. Shear waves in this environment, unlike the P wave, exhibit a strong central lobe. Pulse width measurements examined for a few shear waveforms indicate they are well behaved in rise time plots. The use of shear waves should be emphasized in future applications in the tunnel environment because they are most tractable.

(2) Compressional waves, particularly those generated in a shot hole, can generate significant unwanted other events, particularly SV. Offsets should be adequate to insure the absence of SV contamination in these circumstances. More significant would be the use of a controlled source, such as a vibrator or other mechanical system, which could produce a cleaner P wave source and allow shaping of the source spectrum for near equivalence between sites, thus making comparisons between sites in both the time and frequency domains more unequivocal.

(3) A drift is difficult to find in Rainier Mesa without

cultural effects which may be more of a concern in waveform contamination than the effects of geologic bedding planes. Within freshly mined regions, which in Rainier Mesa historically are chiefly the stemming regions of newly excavated drifts, invert sensors are probably adequate. At other locations the back may be the most suitable location for sensors, although source locations may involve logistic difficulty. Dispensing with shallow drill holes and grouting sensors to depths of only 0.15 m or so is probably adequate.

(4) Sensors ideally should be accelerometers, however, obtaining adequate amplifiers and sensitivity with such systems entails large expenditures, more than were available for this study. Because of gain limitations and hardware failure we were unable to utilize accelerometers for most of the data obtained in this study. Geophones entail some uncertainty with regard to the adequacy of rise times; they have a finite bandwidth which should be investigated for any rise time study. However, geophones are adequate for spectral ratio and for time-domain amplitude techniques.

(5) Finally, it should be realized that attenuation is a measurement best made in the free field. In an environment of horizontal bedding, it is best applied in a vertical drill hole. The desirability of sampling the stemming region at tunnel sites requires horizontal sampling to sample the proper lithology. The free field requirement may be met by use of a horizontal hole, such as the free field hole presently drilled beneath proposed device locations. The expense of this approach should await additional experience with in-tunnel methods. Alternately, but less desirable because of limitations on range and number of detectors employable, might be the use of sensors in the cross cuts between the main and bypass drifts.

REFERENCES CITED

Azimi, S.A., Kalinin, A.V., Kalinin, V.V., and Pivovarov, B.L., 1968, Impulse and transient characteristics of media with linear and quadratic absorption laws: Izvestiya Academy Science USSR Physics of the Solid Earth, no. 2, p. 88-93.

Badri, M., and Mooney, H.M., 1987, Q measurements from compressional seismic waves in unconsolidated sediments: Geophysics, v. 52, no. 6, p. 772-784.

Blair, D.P., and Spathis, A.T., 1982, Attenuation of explosion-generated pulse in rock masses: Journal of Geophysical Research, v. 87, no. B5, p. 3885-3892.

_____ 1984, Seismic source influence in pulse attenuation studies: Journal of Geophysical Research, v. 89, no. B11, p. 9253-9258.

Bourbie, T., Coussy, O., and Zinszner, B., 1987, Acoustics of porous media: Houston, Gulf Publishing Co., 334 p.

Carroll, R.D., 1983, Seismic velocity and postshot properties in and near chimneys: Monterey Containment Symposium, Los Alamos National Laboratory Report LA-9211-C, Monterey, Calif., 1981, Proceedings, p. 379-396.

_____ 1989, Density logging and density of rocks in Rainier Mesa area, Nevada Test Site, Nevada: U.S. Geological Survey Open-File Report 89-329, 72 p., 5 pl., 180-p. appendix.

Carroll, R.D., and Kibler, J.E., 1983, Sourcebook of locations of geophysical surveys in tunnels and horizontal holes including results of seismic refraction surveys, Rainier Mesa, Aqueduct Mesa, and Area 16, Nevada Test Site: U.S. Geological Survey Open-File Report 83-399, 85 p.

Carroll, R.D., and Magner, J.E., 1988, Velocity logging and seismic velocity of rocks in the Rainier Mesa area, Nevada Test Site, Nevada: U.S. Geological Survey Open-File Report 88-380, 85 p., 9 pl., 152-p. appendix.

_____, 1993, A portable vacuum hammer seismic source for use in tunnel environments: U.S. Geological Survey Open-File Report 93-187, 38 p.

Ellis, W.L., and Magner, J.E., 1980, Compilation of results of three-dimensional stress determinations made in Rainier and Aqueduct Mesas, Nevada Test Site, Nevada: U.S. Geological Survey Open-File Report 80-1098, 27 p.

Gladwin, M.T., and Stacey, F.D., 1974, Anelastic degradation of acoustic pulses in rock: Physics of the Earth and Planetary Interiors, v. 8, p. 332-336.

Hamilton, E.L., 1972, Compressional-wave attenuation in marine sediments: Geophysics, v. 37, no. 4, p. 620-646.

Hatherly, P.J., 1986, Attenuation measurements on shallow seismic refraction data: Geophysics, v. 51, no. 2, p. 250-254.

Hoover, D.L., and Magner, J.E., 1990, Geology of the Rainier Mesa-Aqueduct Mesa tunnel areas--U12n tunnel: U.S. Geological Survey Open-File Report 90-623, 51 p.

Johnston, D.H., and Toksöz, M.N., 1980, Ultrasonic P and S wave attenuation in dry and saturated rocks under pressure: Journal of Geophysical Research, v. 85, no. B2, p. 925-936.

Jones, T., 1983, Wave propagation in porous rocks and models for crystal structure, Ph.D. dissertation, Stanford University, Stanford, California.

Jongmans, D., 1990, In-situ attenuation measurements in soils: Engineering Geology, v. 29, p. 99-118.

_____ 1991, Near-source pulse propagation: application to Q-determination: Geophysical Prospecting, v. 39, no. 7, p. 943-952.

Kjartansson, E., 1979, Constant Q-wave propagation and attenuation: Journal of Geophysical Research, v. 84, p. 4737-4748.

Liu, Hsi-Ping, 1988, Effect of source spectrum on seismic attenuation measurements using the pulse-broadening method: Geophysics, v. 53, no. 12, p. 1520-1526.

McDonal, F.J., Angona, F.A., Mills, R.L., Sengbush, R.I., Van Nostrand, R.G., and White, J.E., 1958, Attenuation of shear and compressional waves in Pierre Shale: Geophysics, v. 23, p. 421-439.

McKenzie, C.K., Stacey, G.P., and Gladwin, M.T., 1982, Ultrasonic characteristics of a rock mass: International Journal of Rock Mechanics and Mining Sciences, v. 19, p. 25-30.

Murphy, B.J., and Rosenbaum, M.S., 1989, Attenuation from seismic refraction surveying as a ground investigation aid: Quarterly Journal of Engineering Geology, v. 22, p. 81-86.

Murphy, W.F., III, 1982, Effects of partial water saturation on attenuation in sandstones: Journal of Acoustical Society of America, v. 71, p. 1458-1468.

____ 1984a, Sonic and ultrasonic velocities: Theory versus experiments: Geophysical Research Letters, v. 12, no. 2, p. 85-88.

____ 1984b, Acoustic measures of partial gas saturation in tight sandstones: Journal of Geophysical Research, v. 89, no. B13, p. 11549-11559.

Newman, P.J., and Worthington, M.H., 1982, In-situ investigation of seismic body wave attenuation in heterogeneous media: Geophysical Prospecting, v. 30, no. 4, p. 377-400.

Nur, Amos; Walls, J.D., Winkler, Kenneth, De Vilbiss, J., 1980, Effects of fluid saturation on waves in porous rock and relations to hydraulic permeability: Society of Petroleum Engineers Journal, p. 450-458.

O'Connell, R.J., and Budiansky, B., 1977, Viscoelastic properties of fluid-saturated cracked solids: Journal of Geophysical Research, v. 82, p. 2022-2034.

Petersen, Edward; Rimer, Norton; Nilson, Robert; Profer, William; and Lie, Kay; 1993, Containment Support Program: Defense Nuclear Agency Report DNA-TR-92-158, 124 p.

Redpath, B.B., Edwards, R.B., Hale, R.J., and Kintzer, F.C., 1982, Development of field techniques to measure damping values for near-surface rocks and soils: prepared for the National Science Foundation Earthquake Hazards Mitigation Grant no. PFR-7900192, URS/John A. Blume and Associates, Engineers, San Francisco, California.

Stacey, F.D., Gladwin, M.T., McKavanagh, B., Linde, A.T., and Hastie, L.M., 1975, Anelastic damping of acoustic and seismic pulses: Geophysical Surveys, v. 2, p. 133-151.

Stewart, R.C., 1984, Q and the rise and fall of a seismic pulse: Geophysical Journal of the Royal Astronomical Society, v. 76, p. 793-805.

Strick, E., 1970, A predicted pedestal effect for pulse propagation in constant-Q solids: Geophysics, v. 35, p. 387-403.

Tarif, P., and Bourbie, T., 1987, Experimental comparison between spectral ratio and rise time techniques for attenuation measurement: Geophysical Prospecting, v. 35, no. 6, p. 668-680.

Thordarson, William, 1965, Perched ground water in zeolitized-bedded tuff, Rainier Mesa and vicinity, Nevada Test Site, Nevada: U.S. Geological Survey Report TEI-862, 90 p.

Toksoz, M.N., and Johnston, D.H., 1981, eds., Seismic wave attenuation: Society of Exploration Geophysics, Geophysics Reprint Series, v. 2.

Toksoz, M.N., Johnston, D.H., and Timur, A., 1979, Attenuation of seismic waves in dry and saturated rocks: I. Laboratory measurements: Geophysics, v. 44, p. 681-690.

Tonn, Rainer, 1989, Comparison of seven methods for the computation of Q: Physics of the Earth and Planetary Interiors, v. 55, p. 259-268.

White, R.E., 1992, The accuracy of estimating Q from seismic data: Geophysics, v. 57, no. 11, p. 1508-1511.

Winkler, Kenneth, and Nur, Amos, 1979, Pore fluids and seismic attenuation in rocks: Geophysical Research Letters, v. 6, no. 1, 4 p.

Wright, C., and Hoy, D., 1981, A note on pulse broadening and anelastic attenuation in near-surface rocks: Physics of the Earth and Planetary Interiors, v. 25, p. 1-8.

APPENDIX A

Plots of the raw and reduced data obtained at each site are presented at the end of this appendix. Data pertinent to individual sites follow.

U12p.04 Line 1

The data plots are shown on figures A1-A7 and A22-A28. Reduction of the data for this site was fairly straightforward. Shear-wave data were obtained from geophone arrivals and the P wave data from accelerometers. Accelerometer gains were barely adequate for the far stations, prompting the use of a different type of accelerometer at the N tunnel site. The low signal to noise at the farthest detector resulted in its rejection in obtaining Qp by the spectral ratio technique. A time delay of 15% of the total window was used in acquiring the S wave data in the field. This delay was subtracted to obtain the time-distance plot.

U12p.04 Line 2

The data plots are shown on figures A8-A14 and A 29-A31. The P wave data for this line are poorly developed beyond the first half cycle. Consequently reductions of the P wave data are only presented for the rise time and time-domain amplitude techniques. The invert of this portion of the drift was covered with grout several cm thick at the time of the measurements. Laboratory measurements on three samples of the grout indicate a P-wave velocity of over 3400 m/s. However, the compressional velocity of 3016 m/s obtained along this line is similar to the velocity measured by Raytheon over the same interval prior to placing the grout. Some interaction, possibly due to the presence of the grout, is obviously affecting the P-wave data beyond the first half cycle. The S-wave data, which were generated by an impact source, are not discernibly affected.

The generation of strong SV energy when using a dynamite source, a frequent occurrence in seismic refraction investigations in Rainier Mesa tunnels, is particularly evident on the record on figure A29.

U12n.05 Utilities drift

The data from this site are shown on figures A15-A20 and A32-A38. Several of the accelerometers on this line failed, probably due to shorting of the high impedance by moisture. Both the P- and S wave data obtained at this site were the most difficult to reduce. Several records were rejected in order to obtain a data set which provided usable spectral ratio relationships. The use of a 150 Hz filter may have resulted in overfiltering the data, and the possibility of interference effects from later arrivals on the waveforms is evident. The time-distance plots (Fig. A15, A32) of the "raw" data indicates a sizable delay because a 1 kHz

filter was used during data acquisition in an attempt to reduce noise. This is the only site where data were filtered during acquisition.

Rise Time Data

Table A1 lists the Q values that would be obtained by using the three definitions of pulse broadening shown on figure 14. The rise time defined by Ta and assuming the constant C=0.5 is that most frequently reported in investigations involving this technique. The variance between values suggests some sensitivity to the choice of the definition for pulse broadening. On some traces it is possible that interference effects are impacting Tc. Q values are also presented for value of C=0.285, the value some recommend for use with an impulse velocity source. Because of the uncertainty of the capture of universally clean waveforms at all sites an assessment of the reasons for the variability is not feasible without an expanded data base.

Table A1.--Values of Q derived by rise time technique.

Values of Q by risetime vs arrival time, C=0.5

	Ta		Tb		Tc	
Location	Raw	Fil	Raw	Fil	Raw	Fil
Line 1 Qs	104±15	94±15	25±7	23±1	20±3	27±1
Line 2 Qs	57±25	32±8	15±5	19±6	19±2	47±4
NQs	*	*	*	13±8	31±9	*
Line 1 Qp	23±2	16±4	14±3	4±1	20±5	46±8
Line 2 Qp	34±5	--	17±2	--	25±5	--
NQp	9±2	39±37	5±1	10±5	33±30	32±13

Values of Q by rise time vs arrival time, C=0.298

	Ta		Tb		Tc	
Location	Raw	Fil	Raw	Fil	Raw	Fil
Line 1 Qs	62±9	56±9	15±4	14±1	12±2	16±1
Line 2 Qs	34±15	19±4	9±3	12±4	12±1	28±2
NQs	*	*	*	8±5	19±6	*
Line 1 Qp	14±1	10±2	9±2	3±0	12±3	28±5
Line 2 Qp	21±3	--	10±1	--	15±3	--
NQp	5±1	23±22	3±1	6±3	20±18	19±7

-- No data
* No correlation

TIme Domain Amplitude Data

These data are listed in table A2 for two techniques of reduction, both of which should essentially provide the same result. The two cases are a direct comparison of amplitudes and a comparison of amplitudes referenced to the amplitude at the detector nearest the source. Plots obtained from the two techniques are provided. Q is derived using the dominant frequency indicated by the three methods of defining pulse broadening by assuming they are equivalent to a quarter period. In general, the data generally exhibit consistent values of Q regardless of the method of defining the period, although there is less variability with the amplitude ratio technique.

Table A2.--Values of Q determined by time-domain amplitude techniques.

Amplitude ratio-time domain Q; periods derived from Ta, Tb, Tc

	Ta		Tb		Tc	
Location	Raw	Fil	Raw	Fil	Raw	Fil
Line 1 Qs	28±4	24±3	18±7	13±4	20±10	16±4
Line 2 Qs	25±8	11±3	9±6	8±3	15±1	14±3
NQs	20±9	15±4	10±5	11±5	29±14	18±5
Line 1 Qp	12±5	6±3	5±4	5±2	13±7	10±3
Line 2 Qp	9±4	--	6±3	--	8±4	--
NQp	5±3	2±1	4±4	2±1	6±3	4±2

Amplitude time-domain Q; periods derived from Ta, Tb, Tc

	Ta		Tb		Tc	
Location	Raw	Fil	Raw	Fil	Raw	Fil
Line 1 Qs	29±4	40±10	18±7	22±8	21±10	27±9
Line 2 Qs	24±8	14±4	9±6	10±4	15±1	19±5
NQs	13±5	16±4	7±3	12±6	19±8	20±4
Line 1 Qp	9±4	6±2	4±3	5±2	10±5	10±3
Line 2 Qp	9±4	--	6±3	--	8±4	--
NQp	5±3	3±2	4±3	2±1	6±3	5±3

-- No data

S WAVE DATA FOR P TUNNEL

LINE 1

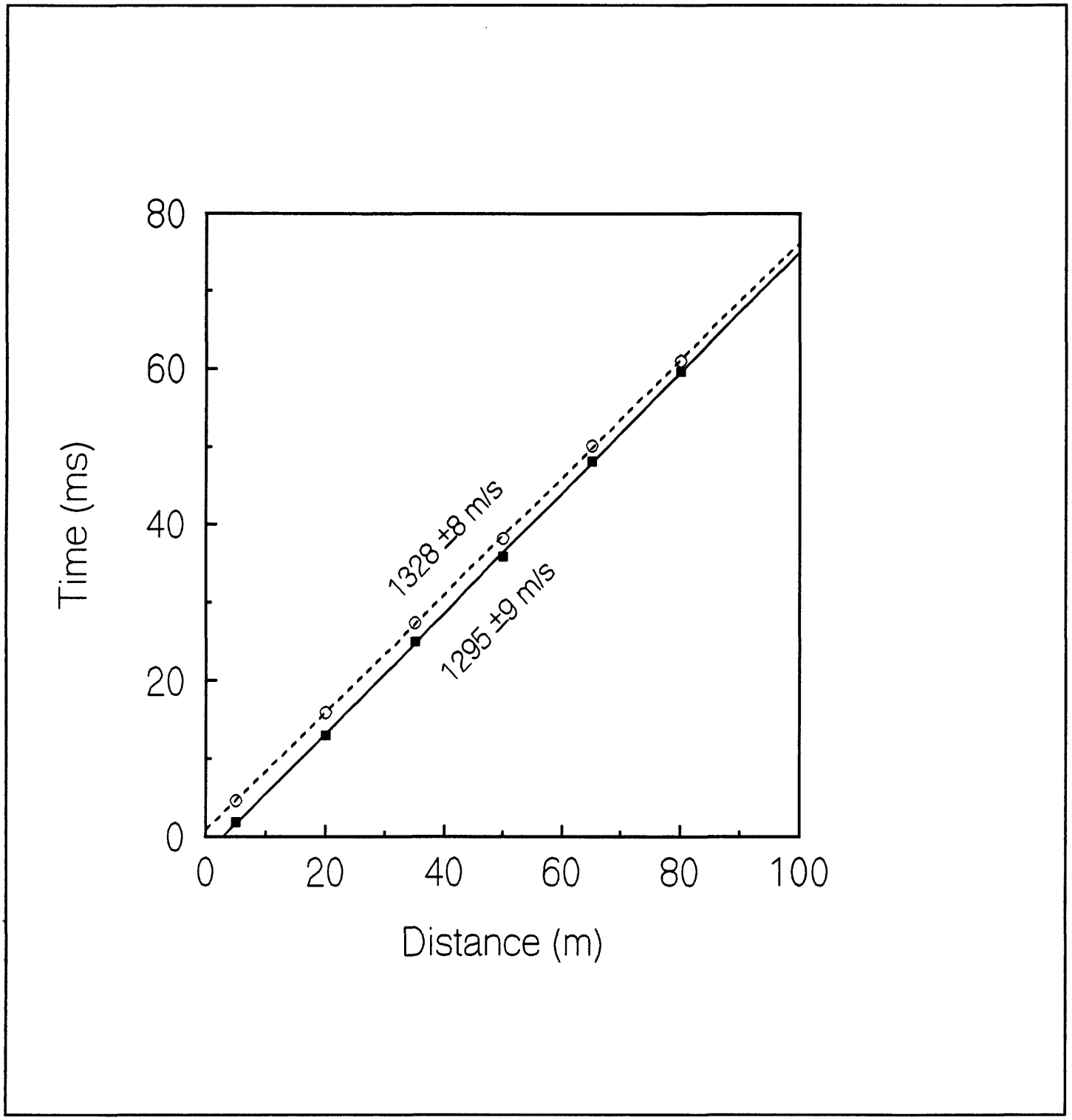

Figure A1.--Shear-wave velocities obtained on Line 1, P04 drift.

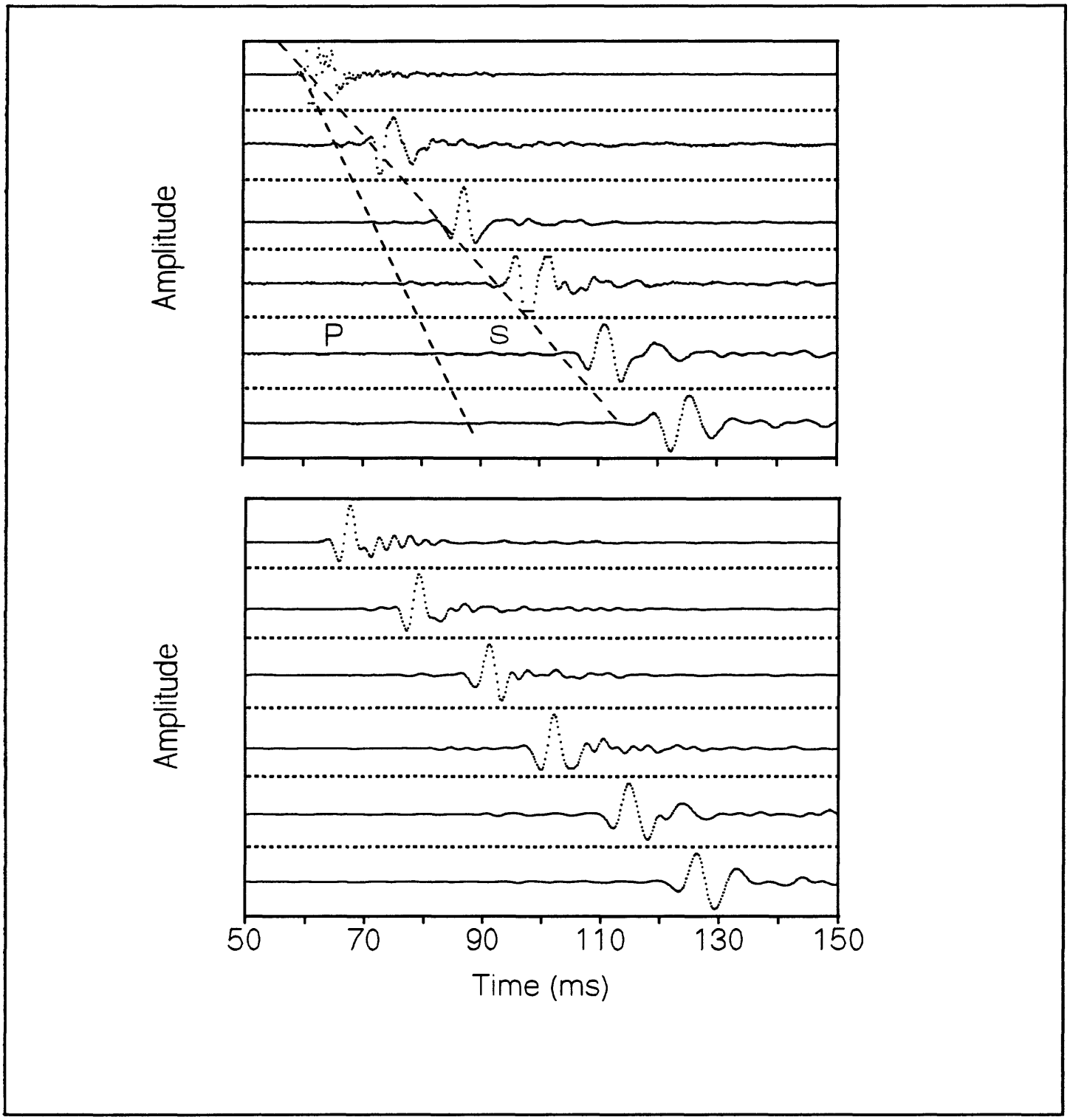

Figure A2.--Unfiltered (top) and 400 Hz filtered (bottom) shear waveforms obtained on Line 1, P04 drift.

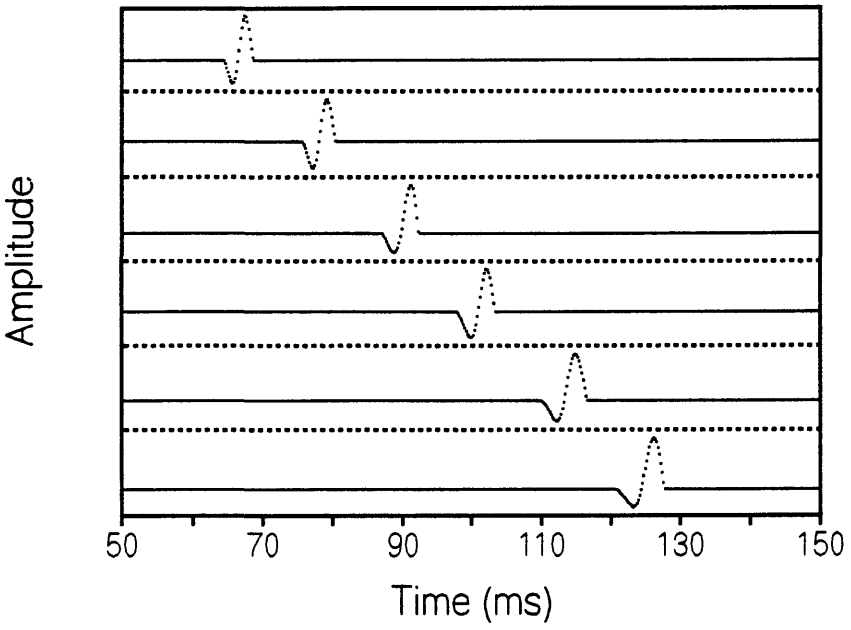

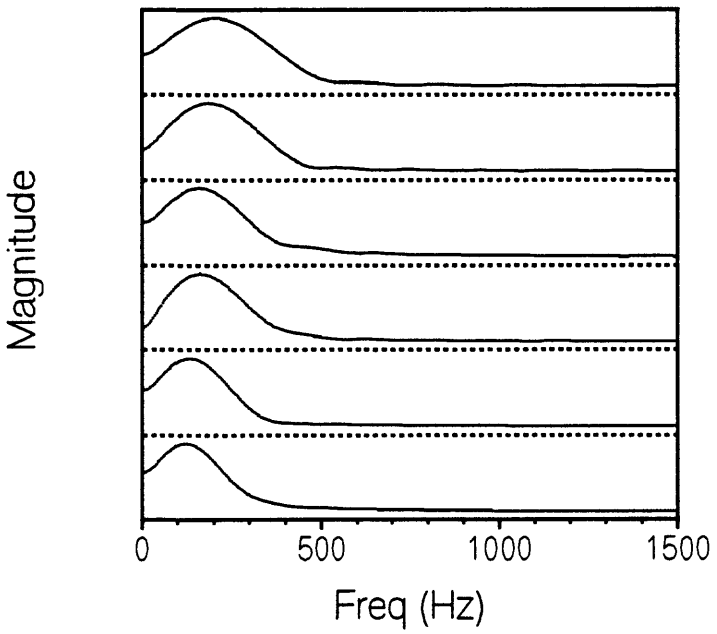

Figure A3.--Extracted shear-wave cycle (top) and FFT (bottom), Line 1, P04 drift.

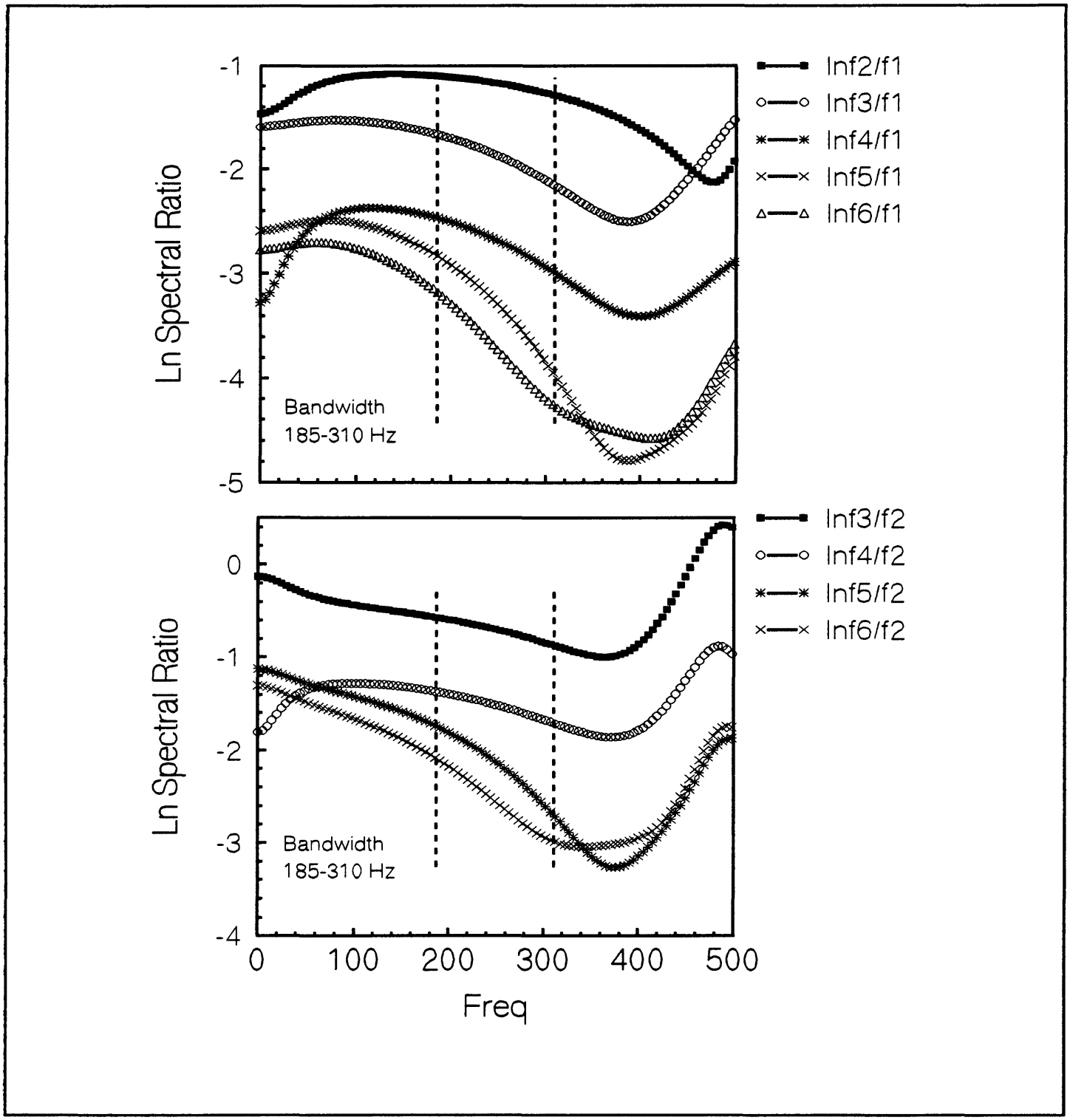

Figure A4.--Spectral ratios for extracted shear-wave cycle using 1st detector (top) and 2nd detector (bottom) as reference. Line 1, P04 drift. Slopes extracted over 185-310 Hz bandwidth.

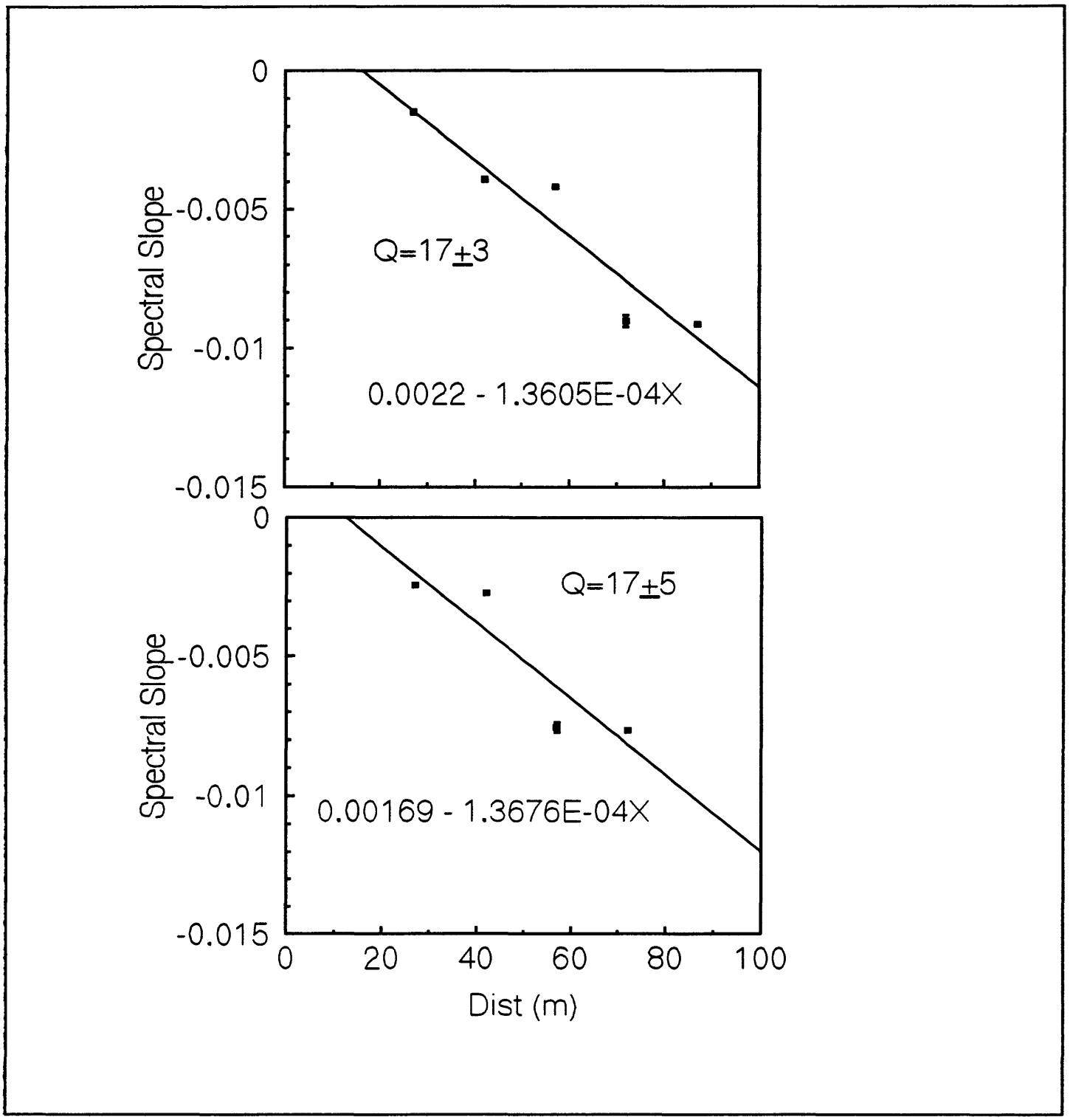

Figure A5.--Spectral slopes versus distance using 1st detector (top) and 2nd detector (bottom) as references. Shear wave, Line 1, P04 drift.